With the use of electrochemical synthetic techniques, we have established that the bridging oxygens in the bis(μ-oxo) core come from water. This information is important since the incorporation of water oxygens into a manganese complex is desirable for water oxidation via such manganese complexes, and it may have implications for the oxygen-evolving complex (OEC) in photosynthetic plants.

Acknowledgment. We owe special thanks to Dr. Melvin P. Klein for his cooperation during the use of his instrumentation for EPR spectroscopy. Also, we wish to thank Dr. F. J. Hollander for the X-ray analysis and many helpful discussions about the results. This work was supported by the Office of Energy Research, Office of Basic Energy Sciences, Division of Chemical Sciences of the U.S. Department of Energy, under Contract DE-AC03-76SF00098.

Registry No. 1, 123567-56-6; $[(14\text{-aneN}_4)\text{MnO}]_2^{2+}$, 117673-54-8; $[(14\text{-aneN}_4)\text{MnO}]_2^{4+}$, 117673-56-0.

Supplementary Material Available: Tables of positional parameters and isotropic thermal parameters, anisotropic thermal parameters, intramolecular distances, intramolecular angles, torsion angles, and root-mean-square amplitudes of thermal vibrations for **1** and a stereoview of **1** (13 pages). Ordering information is given on any current masthead page.

Contribution from the Department of Chemistry,
University of Toronto, Toronto, Ontario, Canada M5S 1A1

Studies of CO Labilization and Intramolecular Hydride Transfer Reactions in Group VI (Cr, Mo, W) Metal-Platinum Heterobimetallic μ-Phosphido Hydrido Carbonyl Complexes

John Powell,* Michael R. Gregg, and Jeffery F. Sawyer

Received February 29, 1988

Oxidative addition of the P-H bond of the secondary phosphine complexes $M(CO)_5(PR_2H)$ (M = Cr, Mo, W; R = Ph, ^{n}Pr) to $Pt(C_2H_4)(PPh_3)_2$ gives $(OC)_5M(\mu\text{-}PR_2)PtH(PPh_3)_2$, which rapidly loses CO (a reversible process) to give $(OC)_4M(\mu\text{-}PR_2)(\mu\text{-}H)Pt(PPh_3)_2$ via a "platinum-assisted mechanism" involving PPh_3 dissociation, formation of a μ-carbonyl intermediate $(OC)_4M(\mu\text{-}PR_2)(\mu\text{-}CO)PtH(PPh_3)$, subsequent rearrangement to $(OC)_4M(\mu\text{-}PR_2)(\mu\text{-}H)Pt(CO)(PPh_3)$, and substitutional loss of CO from Pt (by PPh_3). The complexes $(OC)_4M(\mu\text{-}PPh_2)(\mu\text{-}H)Pt(PR_3)_2$ (PR_3 = PEt_3, PMe_2Ph) can be obtained from the reaction of $M(CO)_5(PPh_2Li)$ and *trans*-$PtHCl(PR_3)_2$. Reaction of $M(CO)_5(PPh_2H)$ with $Pt(1,5\text{-}COD)_2$ in the presence of ethylene gives $(OC)_5M(\mu\text{-}PPh_2)PtH(COD)$, which rapidly rearranges, via β-H transfer, to the complex $(OC)_4M(\mu\text{-}PPh_2)(\mu\text{-}CO)Pt(\eta^3\text{-cyclooctenyl})$. Addition of $M(CO)_5(PPh_2H)$ to $Pt(C_2H_4)_2(PCy_3)$ gives the complexes $(OC)_4M(\mu\text{-}PPh_2)(\mu\text{-}H)Pt(CO)(PCy_3)$ while reaction of *cis*-$(OC)_4M(PEt_3)(PPh_2H)$ (M = Mo, W) with $Pt(C_2H_4)_2(PCy_3)$ gives *mer*-$(OC)_3(PEt_3)M(\mu\text{-}PPh_2)(\mu\text{-}CO)PtH(PCy_3)$. For M = Mo this μ-carbonyl terminal-hydrido complex equilibrates with a small amount of the μ-hydrido terminal-carbonyl isomer *fac*-$(OC)_3(PEt_3)Mo(\mu\text{-}PPh_2)(\mu\text{-}H)Pt(CO)(PCy_3)$. The molecular structure of the complexes $(OC)_4Cr(\mu\text{-}PPh_2)(\mu\text{-}H)Pt(PEt_3)_2$ and $(OC)_4Cr(\mu\text{-}PPh_2)(\mu\text{-}CO)Pt(\eta^3\text{-cyclooctenyl})$ (contains a semibridging carbonyl ligand) have been determined by single-crystal X-ray diffraction methods. The complex $(OC)_4Cr(\mu\text{-}PPh_2)(\mu\text{-}H)Pt(PEt_3)_2$ crystallizes in the space group *Cc* with a = 16.719 (9) Å, b = 11.468 (3) Å, c = 18.275 (6) Å, β = 113.68 (3)°, V = 3209 Å^3, and Z = 4. The structure was refined to R = 0.0346 and R_w = 0.0401 for the 3801 reflections with $I > 3\sigma(I)$. Corresponding data for $(OC)_4Cr(\mu\text{-}PPh_2)(\mu\text{-}CO)Pt(\eta^3\text{-cyclooctenyl})$ are space group $P2_1/a$, a = 25.212 (3) Å, b = 10.172 (2) Å, c = 9.577 (2) Å, β = 90.53 (1)°, V = 2456 Å^3, and Z = 4. R = 0.0329, R_w = 0.0382 for 3384 reflections with $I > 3\sigma(I)$.

Introduction

The recently developed isolobal theory has provided considerable rationalization and proved to be a useful synthetic guide in the field of heterometallic compounds.[1,2] Furthermore the stereochemical "signposting" available in heterometallic systems has considerable potential for the investigation and analysis of cluster assembly and rearrangement processes, for the study of ligand reactivities in multimetallics systems, and for an analysis of the way(s) in which the chemistry of one metal center may be modified by a second metal center in close proximity.[3-13] In this regard systems containing hydrido and phosphine ligands and a platinum atom are particularly amenable to NMR spectroscopic investigation.[14] A suitable entry into heterometallic systems with these features involves oxidative addition of the P-H bond of a secondary phosphine complex to zerovalent complexes of platinum as outlined in Scheme I.[15-17] This reaction has broad potential applicability

Scheme I

$$L_xM(YR_2H) + PtL'_2L'' \longrightarrow L_xM(\mu\text{-}YR_2)PtHL'_2 + L''$$

(eg Y = P, As, Si)

---

(1) Stone, F. G. A. *Angew. Chem., Int. Ed. Engl.* **1984**, *23*, 89.

(2) For recent reviews of mixed-metal compounds see: (a) Roberts, D. A.; Geoffroy, G. L. In *Comprehensive Organometallic Chemistry*; Wilkinson, G., Stone, F. G. A., Abel, E. W., Eds.; Pergamon: Oxford, England, 1982; Chapter 40. (b) Gladfelter, W. L.; Geoffroy, G. L. *Adv. Organomet. Chem.* **1980**, *18*, 207. (c) Langenbach, H. J.; Vahrenkamp, H. *Chem. Ber.* **1979**, *112*, 3773.

(3) Casey, C. P.; Bullock, R. M. *Organometallics* **1984**, *3*, 1100.

(4) Mercer, W. C.; Geoffroy, G. L.; Rheingold, A. L. *Organometallics* **1985**, *4*, 1418.

(5) Chaudret, B.; Dahan, F.; Saba, S. *Organometallics* **1985**, *4*, 1490.

(6) Regragui, R.; Dixneuf, P. H.; Taylor, N. J.; Carty, A. J. *Organometallics* **1984**, *3*, 814.

(7) Sonnenberger, D.; Atwood, J. D. *J. Am. Chem. Soc.* **1980**, *102*, 3484.

(8) Guesmi, S.; Suss-Fink, G.; Dixneuf, P. H.; Taylor, N. J.; Carty, A. J. *J. Chem. Soc., Chem. Commun.* **1984**, 1606.

(9) Fox, J. R.; Gladfelter, W. L.; Geoffroy, G. L. *Inorg. Chem.* **1980**, *19*, 2574.

(10) Fox, J. R.; Gladfelter, W. L.; Wood, T. G.; Smegal, J. A.; Foreman, T. K.; Goeffroy, G. L.; Tavanaiepour, I.; Day, V. W.; Day, C. S. *Inorg. Chem.* **1981**, *20*, 3214.

(11) Planalp, R. P.; Vahrenkamp, H. *Organometallics* **1987**, *6*, 492.

(12) Delavaux, B.; Chaudret, B.; Dahan, F.; Poilblanc, R. *Organometallics* **1985**, *4*, 935.

(13) Rosenberg, S.; Whittle, R. R.; Geoffroy, G. L. *J. Am. Chem. Soc.* **1984**, *106*, 5934.

(14) Moore, D. S.; Robinson, S. D. *Chem. Soc. Rev.* **1983**, *12*, 415.

(15) Powell, J.; Gregg, M. R.; Sawyer, J. F. *J. Chem. Soc., Chem. Commun.* **1984**, 1149.

Table I. Spectroscopic Data for $(OC)_5M(\mu\text{-}PPh_2)PtH(L)_2$ (**2a–c** $[(L)_2 = (PPh_3)_2]$, **2j–l** $[(L)_2 =$ diphos$]$, **5** $[(L_2) = (^nBuNC)(PPh_3)$ with ^nBuNC trans to H], and **7a** $[(L)_2 = 1,5\text{-COD}]$)[a]

compd (M)	IR data, ν(CO),[b] cm^{-1}	^{1}H NMR data for the hydrido ligand (δ, ppm; J, Hz)[c]					^{31}P {^{1}H} NMR data (δ, ppm; J, Hz)[c]								
		δ(H)	$J_{P_\mu-H}$	J_{P_c-H}	J_{P_t-H}	$J_{^{195}Pt-H}$	$\delta(P_\mu)$	$\delta(P_t)$	$\delta(P_c)$	$J_{P_\mu-P_c}$	$J_{P_\mu-P_t}$	$J_{P_c-P_t}$	J_{Pt-P_μ}	J_{Pt-P_c}	J_{Pt-P_t}
2a (Cr)	2049 (w), 1925 (vs, br)	−5.23	19.4	19.4	165	853	*d*								
2b (Mo)	2064 (w), 1930 (vs, br)	−5.17	19.8	19.8	164	856	*d*								
2c (W)	2057 (w), 1902 (vs, br)	−5.20	18	22	167	850	−8[e]	19	24	260	14	15	1530	2330	2330
2j (Cr)	2045 (w), 1921 (vs, br)	−2.86	12	23	164	1023	27	51	49	268	12	0	1877	2013	2165
2k (Mo)	2058 (w), 1927 (vs, br)	−2.90	12	22	175	1034	17	53	51	259	12	0	1780	1985	2144
2l (W)	2061 (w), 1923 (vs, br)	−2.89	12	21	177	1034	−2[e]	52	43	268	12	0	1836	3366	2156
5 (W)	2057 (w), 1920 (vs, br) 2205 (ν(C≡N))	−6.24	12	15		900	−2[e]	22		267			1793	2242	
7a (Cr)[f]	2050 (w), 1925 (vs, br)	−7.45	17			1388	*d*								

[a] Key: P_μ, bridging phosphido; P_c, phosphine ligand cis to H; P_t, phosphine ligand trans to H. [b] CH_2Cl_2 solution. [c] CD_2Cl_2 solution. [d] Complexes **2a,b** and **6a** were too short-lived in solution to obtain well-resolved ^{31}P NMR data. [e] $J_{P-^{183}W}$ not resolved. [f] ^{1}H NMR data for olefinic protons of 1,5-COD ligand in **7a**: δ 4.58 ($J_{PtH} = 36$), 5.78 ($J_{PtH} = 54$).

as illustrated by its use to generate μ-arsenido[18] and μ-silylene complexes.[19] Subject to the P–H bond of L_xMPR_2H being sufficiently acidic to undergo reactions of the type outlined in Scheme I, this approach provides access to a range of easily studied and chemically reactive systems. Thus for example oxidative addition of $M(CO)_5(PPh_2H)$ (**1a–c**; M = Cr, Mo, W)[20] to $Pt(C_2H_4)(PPh_3)_2$ gives initially the μ-phosphido terminal-hydrido platinum complexes $(OC)_5M(\mu\text{-}PPh_2)PtH(PPh_3)_2$ (**2a–c**) (eq 1).

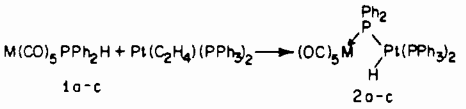

(1)

These molecules contain a group VI metal carbonyl (which has a well-defined mononuclear chemistry in the form of $M(CO)_5(PR_3)$ systems[21,22]) held by a μ-PR_2 group in close proximity to a planar platinum(II) hydride (which also has a well-defined mononuclear chemistry[23]). By virtue of the three donor phosphine ligands and the overall neutrality of the system, it was felt that the hydride ligand of **2** may be more hydridic, and hence more reactive, relative to other platinum(II) hydrides of the type $PtHX(PR_3)_2$. In this paper, we report the synthesis of complexes of type **2** that undergo facile CO loss to give the μ-hydrido complexes **3** (eq 2). Evidence is presented to show that this "net substitution" of CO at the group VI metal center of **2** by the hydride ligand on platinum to give **3** is "platinum assisted", occurring via PR_3 dissociation from the platinum and CO transfer via a μ-CO to the platinum prior to actual loss of CO from the molecule. Additional information supporting this proposal was obtained from a study of the reactions of $M(CO)_5(PR_2H)$ and *cis*-$Mo(CO)_4(PEt_3)(PPh_2H)$ with $Pt(C_2H_4)_2(PCy_3)$ and $Pt(COD)_2$ (COD = *cis,cis*-1,5-cyclooctadiene). The data provide a well-defined example of the way in which a "16e metal center" may influence the chemistry of an adjacent "18e metal center" in heterobimetallic compounds. X-ray structural studies of $(OC)_4Cr(\mu\text{-}PPh_2)(\mu\text{-}H)Pt(PEt_3)_2$ and $(OC)_4Cr(\mu\text{-}PPh_2)(\mu\text{-}CO)Pt(\eta^3\text{-cyclooctenyl})$ (a molecule containing an unsymmetrical CO bridge) are also reported.

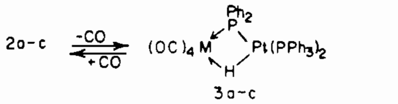

(2)

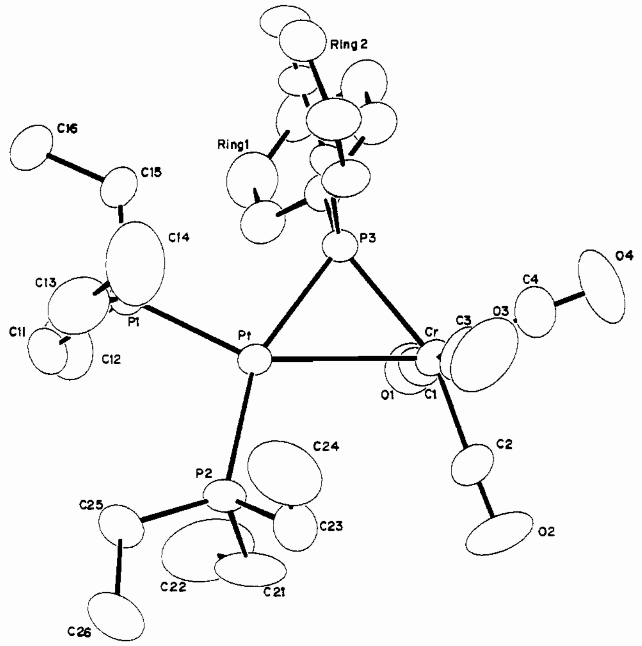

Figure 1. Molecular structure of $(OC)_4Cr(\mu\text{-}PPh_2)(\mu\text{-}H)Pt(PEt_3)_2$ (**3d**) as determined by single-crystal X-ray diffraction. Selected bond lengths (Å): Pt–Cr = 2.905 (2), Pt–P1 = 2.287 (2), Pt–P2 = 2.322 (2), Pt–P3 = 2.321 (2), Cr–P3, = 2.320 (3), Cr–C1 = 1.877 (12), Cr–C2 = 1.819 (10), Cr–C3 = 1.864 (10), Cr–C4 = 1.815 (12). Selected bond angles (deg): P1–Pt–P2 = 101.5, P1–Pt–P3 = 102.0. P3–Pt–Cr = 51.2, Cr–Pt–P1 = 153.2, P3–Cr–Pt = 51.2, Pt–Cr–C1 = 92.8, Pt–Cr–C2 = 109.3, Pt–Cr–C3 = 94.1, Pt–Cr–C4 = 157.0. The position of the bridging hydride ligand is assumed to be approximately trans to P1 and C4.

Results

Reaction of $M(CO)_5(PPh_2H)$ with $Pt(C_2H_4)(PPh_3)_2$. The secondary-phosphine complexes $M(CO)_5(PPh_2H)$ (**1a–c**; M = Cr (**1a**), Mo (**1b**), W (**1c**))[20] were prepared under mild conditions following the method described by Schenk[24] for the synthesis of $M(CO)_5(PR_3)$. In CH_2Cl_2 solution, **1a–c** oxidatively add to $Pt(C_2H_4)(PPh_3)_2$ to give the bridging-phosphido terminal-hydrido complexes $(OC)_5M(\mu\text{-}PPh_2)PtH(PPh_3)_2$ (**2a–c**) (eq 1) (see Table I for ^{1}H and ^{31}P{^{1}H} NMR and IR data). The observed ν(CO) data for **2a–c** are ca. 10–20 cm^{-1} lower than those for the corresponding **1a–c** compounds and suggest that "$PPh_2[PtH(PPh_3)_2]$" is a more basic ligand than PPh_2H. The formation of the cis isomer **2a–c**, rather than the trans isomer, is presumably a consequence of the large steric bulk (cone angle) of the "$PPh_2[M(CO)_5]$" moiety that favors its location cis to the small hydrido ligand on Pt. The relative rates of formation of **2** (as determined by IR spectroscopy) decrease in the order $W(CO)_5(PPh_2H)$ > $W(CO)_5(P^nPr_2H)$ ≫ $W(CO)_5(PCy_2H)$ [no reaction with Pt-

---

(16) Powell, J.; Sawyer, J. F.; Smith, S. J. *J. Chem. Soc., Chem. Commun.* **1985**, 1312.
(17) Powell, J.; Sawyer, J. F.; Stainer, M. V. R. *J. Chem. Soc., Chem. Commun.* **1985**, 1314; *Inorg. Chem.*, following paper in this issue.
(18) Powell, J.; Phillips, J. Unpublished results.
(19) Powell, J.; Sawyer, J. F.; Shiralian, M. *Organometallics* **1989**, *8*, 577.
(20) Treichel, P. M.; Dean, W. K.; Douglas, W. M. *J. Organomet. Chem.* **1972**, *42*, 145.
(21) Darensbourg, D. J. *Adv. Organomet. Chem.* **1982**, *21*, 112.
(22) Dobson, G. R.; Hodges, P. M.; Healy, M. A.; Poliakoff, M.; Turner, J. J.; Firth, S.; Asali, K. J. *J. Am. Chem. Soc.* **1987**, *109*, 4218.
(23) Hartley, F. R. *The Chemistry of Platinum and Palladium*; Wiley: New York, 1973; Chapter 4.
(24) Schenk, W. A. *J. Organomet. Chem.* **1979**, *179*, 253.

Table II. Analytical and Spectroscopic Data for Complexes $(OC)_4M(\mu\text{-}PPh_2)(\mu\text{-}H)Pt(PR_3)(PR'_3)$ (**3a–o**)

complex				elem anal., % calcd (found)		IR ν(CO) region,[b] cm^{-1}				^{1}H NMR data for the hydrido ligand (δ, ppm; J, Hz)[c]					
	M	PR_3	PR'_3	C	H					δ(H)	$J_{P_\mu\text{-}H}$	$J_{P_c\text{-}H}$	$J_{P_t\text{-}H}$	$J_{^{195}Pt\text{-}H}$	$J_{^{183}W\text{-}H}$
3a	Cr	PPh_3	PPh_3	58.4 (58.05)	3.8 (3.8)	1992 s	1895 m	1878 vs	1857 m	−11.0	27	17	107	648	
3b	Mo	PPh_3	PPh_3	56.1 (56.1)	3.7 (3.7)	2006 s		1892 vs, br	1856 m	−9.0	29	15	114	679	
3c	W	PPh_3	PPh_3	52.0 (51.8)	3.4 (3.25)	2002 s	1899 m	1881 vs	1864 m	−7.9	30	14	111	668	30
3d	Cr	PEt_3	PEt_3	43.0 (42.6)	5.2 (5.1)	1991 s	1895 m	1878 vs	1844 m	−12.8	25	15	103	587	
3e	Mo	PEt_3	PEt_3	40.8 (40.5)	5.0 (5.1)	2006 s	1901 m	1892 vs	1845 m	−10.5	29	18	109	640	
3f	W	PEt_3	PEt_3	36.8 (36.8)	4.5 (4.5)	2002 s	1892 m	1881 vs	1841 m	−9.8	27	13	101	615	30
3g	Cr	PMe_2Ph	PMe_2Ph	46.8 (46.3)	4.0 (4.0)	1991 s	1895 m	1878 vs	1855 m	−12.0	24	18	105	620	
3h	Mo	PMe_2Ph	PMe_2Ph	44.4 (44.2)	3.8 (3.8)	2006 s		1900 vs, br	1850 m	−10.0	29	15	112	670	
3i	W	PMe_2Ph	PMe_2Ph	40.3 (40.4)	3.5 (3.7)	2002 s	1899 m	1880 vs	1850 m	−9.2	26	12	105	656	30
3j	Cr	diphos		53.5 (53.4)	3.7 (3.7)	1992 s	1898 s	1883 vs	1858 m	−9.5	17	14	105	693	
3k	Mo	diphos		51.1 (51.4)	3.5 (3.4)	2006 s	1904 s	1892 s	1860 m	−7.6	14	14	112	752	
3l	W	diphos		46.9 (47.0)	3.3 (3.5)	2002 s	1895 s	1884 s	1856 m	−6.9	15	11	106	720	25
3m	Cr	PPh_2H	PCy_3			1993 s	1893 s	1882 s	1845 m	−11.5	19	19	110	686	
3n	Mo	PPh_2H	PCy_3	52.4 (52.2)	5.2 (5.5)	2007 s	1903 s	1888 s	1850 m	−9.4	22	12	115	737	
3o	W	PPh_2H	PCy_3	48.3 (48.9)	4.5 (5.4)	2004 s	1893 s	1882 s	1844 m	−8.1	24	8	112	720	nr

	$^{31}P\{^1H\}$ NMR data (δ, ppm; J, Hz)[b]									
complex	$\delta(P_\mu)$	$\delta(P_c)$	$\delta(P_t)$	$J_{P_\mu\text{-}P_c}$	$J_{P_\mu\text{-}P_t}$	$J_{P_c\text{-}P_t}$	$J_{^{195}Pt\text{-}P_\mu}$	$J_{^{195}Pt\text{-}P_c}$	$J_{^{195}Pt\text{-}P_t}$	$J_{^{183}W\text{-}P_\mu}$
3a	144	11	21	183	18	20	1635	2312	3494	
3b	108	11	18	189	18	19	1462	2210	3413	
3c	100	13	14	191	21	18	1420	2250	3500	198
3d	130	7	9	201	26	19	1580	2256	3224	
3e	107	19	18	196	15	18	1405	2206	3223	
3f	87	1	8	199	19	19	1352	2230	3300	235
3g	132	12	13	196	19	19	1550	2300	3260	
3h	100	12	19	200	19	18	1420	2206	3280	
3i	89	−15	−20	181	18	22	1331	2256	3320	217
3j	118	51	53	192	14	7	1570	2306	3240	
3k	94	46	45	195	14	7	1410	2170	3180	
3l	86	51	46	180	14	8	1360	2230	3305	204
3m	133	31	0.3	170	21	20	985	2400	3257	
3n	97	29	−5	170	21	18	1135	2316	3238	
3o	90	28	−11	169	19	20	1080	2344	3350	nr

[a] Key: P_μ, bridging phosphido; P_c, PR_3 ligand cis to μ-H; P_t, PR'_3 trans to μ-H; nr, not recorded. [b] In CH_2Cl_2. [c] In CD_2Cl_2.

$(C_2H_4)(PPh_3)_2$ at 20 °C]. For $M(CO)_5(PPh_2H)$ the relative rates decrease in the order Cr > Mo > W, which is in the order of decreasing acidity of the P–H bond of $M(CO)_5(PH_3)$[25] [and presumably $M(CO)_5(PPh_2H)$].

On standing, solutions of **2a–c** readily lose CO to give the well-defined crystalline μ-phosphido μ-hydrido complexes $(OC)_4M(\mu\text{-}PPh_2)(\mu\text{-}H)Pt(PPh_3)_2$ (**3a–c**) (eq 2). The triethylphosphine and phenyldimethylphosphine analogues $(OC)_4M(\mu\text{-}PPh_2)(\mu\text{-}H)Pt(PR_3)_2$ [**3d–f** ($PR_3 = PEt_3$), **3g–i** ($PR_3 = PMe_2Ph$)] have been obtained from the reaction of $M(CO)_5(PPh_2Li)$ with *trans*-$PtHCl(PR_3)_2$. (Spectroscopic data are given in Table II.) The molecular structure of the triethylphosphine complex $(OC)_4Cr(\mu\text{-}PPh_2)(\mu\text{-}H)Pt(PEt_3)_2$ (**3d**) as determined by single-crystal X-ray diffraction, is shown in Figure 1 (structural details provided later); the relative rates of formation of **3a–c** from **2a–c** decrease in the order Cr > Mo > W. At 25 °C, the **2** → **3** reaction is >90% complete in 8 min (M = Cr), 15 min (Mo), or 150 min (W). The reaction **2a–c** → **3a–c** is readily reversed within 5 min by bubbling CO (1 atm) through the solution. The complexes $(OC)_4M(\mu\text{-}PPh_2)(\mu\text{-}H)Pt(PR_3)_2$ ($PR_3 = PEt_3$, PMe_2Ph) likewise react rapidly and reversibly with CO to give the terminal hydrides $(OC)_5M(\mu\text{-}PPh_2)PtH(PR_3)_2$ (**2d–i**) [characterized mainly by IR (ν(CO) region)] (eq 3). On removal of CO (N_2 sweep) the bridged hydrides **2c–i** are regenerated. Prolonged CO bubbling (>1 h) through solutions of **3a–c** leads to reductive elimination of $(OC)_5M(PPh_2H)$ from the initially formed **2a–c** and formation of $Pt(CO)_2(PPh_3)_2$.[26] As a possible consequence of the more basic nature of the phosphines, the PEt_3 and Me_2PhP systems **2d–i**/**3d–i** are much less susceptible to reductive elimination on prolongued exposure to CO. In contrast to the monodentate phosphine systems, the complexes $(OC)_5M(\mu\text{-}PPh_2)PtH(dppe)$ (**2j–l**) and $(OC)_4M(\mu\text{-}PPh_2)(\mu\text{-}H)Pt(dppe)$ (**3j–l**) (dppe = 1,2-bis(diphenylphosphino)ethane) interconvert *very slowly*. (N.B. **2j–l** and **3j–l** were obtained from the addition of 1 molar equiv of dppe to **2a–c** or **3a–c**.) Thus, for example, on standing in CD_2Cl_2 at room temperature, $(OC)_5W(\mu\text{-}PPh_2)PtH(dppe)$ (**2l**) rearranges to ca. 20% $(OC)_4W(\mu\text{-}PPh_2)(\mu\text{-}H)Pt(dppe)$ (**3l**) over a period of 4 days. Bubbling CO through a solution **3l** produces no **2l** after 2 h. Reaction of **2c** with an excess of dppe gives $W(CO)_5(PPh_2H)$ and $Pt(dppe)_2$ as the major products.

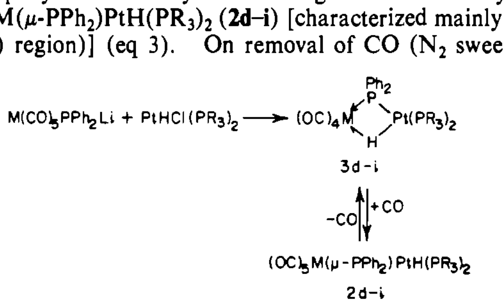

(3)

Addition of the strong π-acid *n*-BuNC to $(OC)_4M(\mu\text{-}PPh_2)(\mu\text{-}H)Pt(PPh_3)_2$ (**3a–c**) readily displaces the PPh_3 trans to the μ-H ligand to give the isocyanide complexes $(OC)_4M(\mu\text{-}PPh_2)(\mu\text{-}H)Pt(n\text{-}BuNC)(PPh_3)$ (**4a–c**) (eq 4) (isolated samples were usually contaminated with small amounts of **3a–c**). Solutions of **4a–c** are unreactive toward added CO (1 atm, room temperature, 2 h). Likewise, addition of *n*-BuNC to **2c** gave $(OC)_5W(\mu\text{-}PPh_2)PtH(n\text{-}BuNC)(PPh_3)$ (**5**; *n*-BuNC trans to terminal H). This complex remained unchanged, with respect to CO loss and possible formation of **4c**, after 2 days in CD_2Cl_2 solution (room temperature).

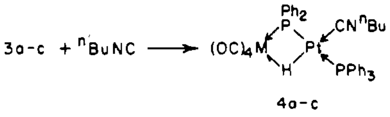

(4)

4a-c

---

(25) Guggenberger, L. S.; Klabunde, U.; Schunn, R. A. *Inorg. Chem.* **1973**, *12*, 1143.

(26) Chatt, J.; Chini, P. *J. Chem. Soc. A* **1970**, 1538.

Table III. Spectroscopic Data for $(OC)_4M(\mu\text{-}PPh_2)(\mu\text{-}H)Pt(CN^nBu)(PPh_3)$ (**4a–c**) and $(OC)_4M(\mu\text{-}PR_2)(\mu\text{-}H)Pt(CO)(PR_3)$ (**6a–c** (μ-PPh_2, PCy_3), **6d–f**, (μ-P^nPr_2, PCy_3), **6g,h** (μ-PPh_2, PPh_3))^a

complex (M)	IR data,^{b} cm^{-1}		^{1}H NMR data for the hydrido ligand (δ, ppm; J, Hz)^c					$^{31}P\{^1H\}$ NMR data^b						elem anal., % calcd (found)	
	ν(CN/CO(Pt))	ν(CO(M))	δ(H)	$J_{P_\mu-H}$	J_{P_c-H}	$J_{^{195}Pt-H}$	$J_{^{183}W-H}$	$\delta(P_\mu)$	$\delta(P_c)$	$J_{P_\mu-P_c}$	$J_{^{195}Pt-P_\mu}$	$J_{^{195}Pt-P_c}$	$J_{^{183}W-P_\mu}$	C	H
4a (Cr)	2191	1997 s, 1887 vs, br, 1856 s, br	−12.3	14.5	14.5	615		141	22	175	1318	2399			
4b (Mo)	2195	2012 s, 1905 vs, br, 1856 s, br	−10.3	18	12	687		105	18	177	1160	2300			
4c (W)	2195	2007 s, 1898 vs, br, 1852 s, br	−9.7	13	13	665	23	97	20	176	1101	1982	207		
6a (Cr)	2067	2005 s, 1909 sh, 1899 vs, 1869 s	−11.2	20	12	688		144	36	131	1136	2228		49.3 (48.5)	5.2 (5.2)
6b (Mo)	2070	2016 s, 1915 vs, br, 1868 s	−9.1	21	9	752		121	48	134	971	2128		46.8 (46.5)	4.9 (4.9)
6c (W)	2069	2012 s, 1903 vs, br, 1863 s	−8.5	21	7	730	25	104	40	133	900	2158	nr	42.7 (42.2)	4.5 (4.3)
6d (Cr)	2058	1998 s, 1886 vs, br, 1862 s	−10.8	22	12	686		153	40	115	1025	2168		44.4 (44.1)	6.1 (6.1)
6e (Mo)	2062	2010 s, 1903 vs, br, 1861 s	−8.4	24	8	758		114	41	121	864			42.0 (40.9)	5.8 (5.6)
6f (W)	2062	2006 s, 1879 vs, br. 1858 s	−7.7	24	6	731	30	98	39	120	814	2156	220	38.0 (37.7)	5.2 (5.2)
6g (Cr)	identified as short-lived intermediates in **2** → **3** reaction by ^{1}H NMR		−10.5	24	12	697									
6h (Mo)	**6g** also obtained on addition of PPh_3 to **7a**		−8.4	16	14	770									

^{a}Key: P_μ, bridging phosphido; P_c, PR_3 ligand cis to μ-H; nr, not recorded. ^{b}CH_2Cl_2 solution. ^{c}CD_2Cl_2 solution.

Table IV. Spectroscopic Data (CD_2Cl_2) for $(OC)_4M(\mu\text{-}PPh_2)(\mu\text{-}CO)Pt(\eta^3\text{-cyclooct-4-en-1-yl})$, (**8a** (M = Cr), **8c** (M = W))^a

complex	elem anal., % calcd (found)		IR data, ν(CO),^{b} cm^{-1}		$^{31}P\{^1H\}$ NMR data (δ, ppm; J, Hz)	
	C	H	terminal CO	semibridging CO	$\delta(P_\mu)$	$J_{^{195}Pt-P_\mu}$
8a	44.1 (44.0)	3.4 (3.3)	2047 s, 1974 sh, 1947 vs, br	1831 m, br	114	3153
8c	37.0 (36.6)	2.8 (2.7)	2062 s, 1985 sh, 1948 vs, br	1857 m, br		

$^{13}C\{^1H\}$ NMR Data (δ, ppm; J, Hz)

complex	carbonyls				cyclooct-4-en-1-yl ligand							
	$\delta(C_c)$	$\delta(C_t)$	$J_{P_\mu-C_c}$	$J_{P_\mu-C_t}$	$\delta(C_1)$	$\delta(C_2)$	$\delta(C_3)$	$\delta(C_4)$	$\delta(C_5)$	$\delta(C_6)$	$\delta(C_7)$	$\delta(C_8)$
8a	220	224	8	12	35	31	42	117	113	26	36	25
8c	202	200	nr	6	33	31	43	115	111	26	36	25

complex	cyclooct-4-en-1-yl ligand											
	$J_{P_\mu-C_1}$	$J_{P_\mu-C_3}$	$J_{P_\mu-C_4}$	$J_{P_\mu-C_5}$	J_{Pt-C_1}	J_{Pt-C_2}	J_{Pt-C_3}	J_{Pt-C_4}	J_{Pt-C_5}	J_{Pt-C_6}	J_{Pt-C_7}	J_{Pt-C_8}
8a	2	4	10	5	692	28	14	60	90	19	45	86
8c	0	4	10	4	710	30	15	69	92	22	40	86

^{a}Key: C_t, carbonyl ligand trans to μ-PPh_2; C_c, carbonyl ligands cis to μ-PPh_2. For C_c, fast-exchange-limit data were used for carbonyls 1, 2, 3, and b; see eq 6 and Scheme II. Data recorded at 20 °C. ^{b}CH_2Cl_2 solution.

Reaction of $M(CO)_5(PR_2H)$ (R = Ph, ^{n}Pr) with $Pt(C_2H_4)_2(PCy_3)$. Oxidative addition of $M(CO)_5(PPh_2H)$ (**1a–c**) and $M(CO)_5(P^nPr_2H)$ [**1d** (Cr), **1e** (Mo), **1f** (W)] to the zerovalent platinum compound $Pt(C_2H_4)_2(PCy_3)$ in CH_2Cl_2, at room temperature, leads quantitatively (as determined spectroscopically) to $(OC)_4M(\mu\text{-}PR_2)(\mu\text{-}H)Pt(CO)(PCy_3)$ (**6a–f**) (eq 5). The reaction is essentially complete in 5 (Cr), 8 (Mo), and 15 min (W) using **1a–c** and a slight excess of $Pt(C_2H_4)_2(PCy_3)$.

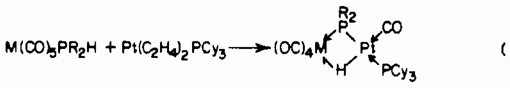

6 a-f

(5)

The addition of a molar equivalent of PPh_2H to $(OC)_4M(\mu\text{-}PPh_2)(\mu\text{-}H)Pt(CO)(PCy_3)$ (**6a–c**) occurs as outlined in eq 6. The immediate products are a mixture of the terminal-hydride $(OC)_5M(\mu\text{-}PPh_2)PtH(PPh_2H)(PCy_3)$ (**2m–o**) (CO migration back to M) and the bridging-hydride $(OC)_4M(\mu\text{-}PPh_2)(\mu\text{-}H)Pt(PPh_2H)(PCy_3)$ (**3m–o**) (simple substitutional loss of CO from M). On standing, **2m–o** (identified by the characteristic ν(CO) pattern in the IR region) quickly rearrange to **3m–o**. The initially formed relative amounts of **2m–o** and **3m–o** are sensitive to the nature of M. For M = Cr, the predominant reaction (eq 6) involves displacement of CO and formation of **3m** (>90%) while, for Mo, the initial ratio of **2n**:**3n** is 65:35 and for W the ratio **2o**:**3o** is 37:63. Similar M-dependent results are obtained when a molar equivalent of PPh_3 is added to **6a–c**.

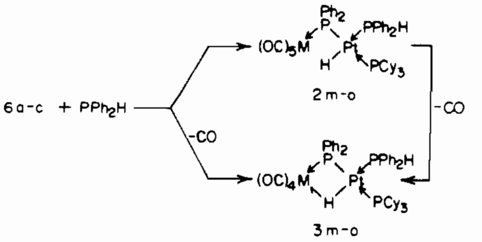

(6)

Characterization of Complexes 2–6. The ^{1}H and $^{31}P\{^1H\}$ NMR and IR spectroscopies (ν(CO) region) provide ready structural characterization, and the relevant data for all the new complexes described herein are listed in Tables I–V. The molecular structure of **3d** was determined by an X-ray diffraction study (see below). The relative magnitude of $J_{^{195}Pt-^1H}$ and $^2J_{^{31}P(\text{trans to H})-^1H}$ for the hydride ligand are diagnostic of the bonding mode[14,27] being >800 and ca. 165 Hz, respectively, for the terminal hydrides (e.g. **2**) (values of 770 and 166 Hz are observed in $[PtH(PPh_3)_3]^+$[28]) and ≤750 and ca 110 Hz for the bridged hydrides (e.g. **3**). Spin–spin coupling of the hydride to ^{31}P(cis ligands) is ca 10–25 Hz. The relative magnitude of $J_{^{183}W-^1H}$ is ca. 30 Hz for bridged hydrides and ca. 0 Hz for terminal hydrides. The $^{31}P\{^1H\}$ NMR data fully support the structures given with $\delta(P_\mu)$ for "$M(\mu\text{-}PR_2)(\mu\text{-}H)Pt$" systems occurring well downfield from the PR_3 resonances while in the singly bridged systems containing "$M(\mu\text{-}PPh_2)Pt$" $\delta(P_\mu)$ occurs upfield of the PR_3 resonances, consistent with previous literature correlations.[29,30]

Reaction of $M(CO)_5(PPh_2H)$ with $Pt(COD)_2$. While complexes **1a–c** are unreactive toward $Pt(COD)_2$, the reaction in hexane solution in the presence of ethylene [known to produce $Pt(C_2H_4)_3$ from $Pt(COD)_2$[31]] results in the rapid precipitation of $(OC)_5M(\mu\text{-}PPh_2)PtH(COD)$ (**7a**, M = Cr; **7c**, M = W) as yellow solids. [Attempts to prepare **7b** (M = Mo) from **1b** were unsuccessful

---

(27) Venanzi, L. M. *Coord. Chem. Rev.* **1982**, *43*, 251.
(28) Dingle, T. W.; Dixon, K. *Inorg. Chem.* **1974**, *13*, 847.
(29) Carty, A. J. *Adv. Chem. Ser.* **1982**, *No. 196*, 1963.
(30) Garrou, P. E. *Chem. Rev.* **1981**, *81*, 229.
(31) Green, M.; Howard, J. A. K.; Spencer, J. L.; Stone, F. G. A. *J. Chem. Soc., Dalton Trans.* **1977**, 271.

Table V. Spectroscopic Data for $(OC)_3(PEt_3)M(\mu\text{-}PPh_2)(\mu\text{-}CO)PtH(PCy_3)$ (**14a,b**) and $(OC)_3(PEt_3)Mo(\mu\text{-}PPh_2)(\mu\text{-}H)Pt(CO)(PCy_3)$ (**15a**)[a]

	elem anal., % calcd (found)		IR data, ν(CO) region, cm^{-1}	
complex (M)	C	H	terminal CO	bridging CO
14a (Mo)	48.7 (48.8)	6.0 (5.9)	2008 (m), 1906 s, br	1750 m, br
14b (W)	44.7 (44.2)	5.5 (5.4)	2004 (m), 1897 s, br	1736 m, br

^{1}H NMR Data for the Hydrido Ligand (δ, ppm; J, Hz)[c]

complex	δ(H)	$J_{P_\mu\text{-}H}$	$J_{P_c\text{-}H}$	$J_{P_M\text{-}H}$	$J_{^{195}Pt\text{-}H}$
14a	−5.5	24	6.4		1264
14b	−6.1	24	5.8		1265
15a	−9.27	19	6.4	12	818

^{31}P{^{1}H} Data (δ, ppm; J, Hz)[b]

complex	$\delta(P_\mu)$	$\delta(P_c)$	$\delta(P_M)$	$J_{P_\mu\text{-}P_c}$	$J_{P_\mu\text{-}P_M}$	$J_{Pt\text{-}P_\mu}$	$J_{Pt\text{-}P_c}$	$J_{Pt\text{-}P_M}$	$J_{W\text{-}P_\mu}$	$J_{W\text{-}P_M}$
14a	101	43	20	200	26	1465	3235	48		
14b	80	45	4	199	21	1410	3292	40	200	240
15a	99	38	16	134	26	948	2107	0		

^{13}C{^{1}H} NMR Data (δ, ppm; J, Hz) for Carbonyl Ligands[c]

complex	$\delta(C_\mu)$	$\delta(C_{ax})$	$\delta(C_{eq})$	$J_{P_\mu\text{-}C_\mu}$	$J_{P_c\text{-}C_\mu}$	$J_{P_M\text{-}C_\mu}$	$J_{Pt\text{-}C_\mu}$	$J_{^{183}W\text{-}C_\mu}$
14a	246	209	217	1.8	0	9.9	260	
14b	239	201	209	6.7	0	6.7	232	93

complex	$J_{P_\mu\text{-}C_{ax}}$	$J_{P_m\text{-}C_{ax}}$	$J_{P_\mu\text{-}C_{eq}}$	$J_{P_M\text{-}C_{eq}}$	$J_{^{183}W\text{-}C_{ax}}$	$J_{^{183}W\text{-}C_{eq}}$
14a	10	10	23	12.5		
14b	7	7	22	9.8	123	130

[a] Key: C_μ, bridging CO; C_{ax} (axial CO; C_{eq} CO trans to μ-P; P_μ, bridging phosphido; P_c, PCy_3 ligand on Pt cis to H and μ-CO; P_M, PEt_3 ligand on M trans to μ-CO. [b] CH_2Cl_2 solution. [c] CD_2Cl_2 solution.

and led to considerable decomposition.] A likely reaction sequence for the formation of **7** is given in eq 7. The structure of **7**, which

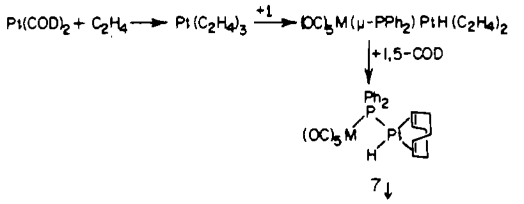

(7)

rapidly rearranges in solution (see below), is based primarily on the IR and ^{1}H NMR data for **7a** (Table I). The carbonyl region exhibits ν(CO) absorptions typical of a $M(CO)_5(PR_3)$ system[21] while in the ^{1}H NMR spectrum a high-field hydridic resonance at δ −7.45 exhibits a $J_{^{195}Pt\text{-}^1H}$ of 1388 Hz, typical of a terminal hydride[14] with a $J_{^{31}P\text{-}^1H}$ of 17 Hz being typical of coupling to a cis phosphine moiety. On dissolving in CH_2Cl_2, the complexes $(OC)_5M(\mu\text{-}PPh_2)PtH(COD)$ (**7a,c**) rearrange within minutes (20 °C) via a presumed β-H-transfer mechanism to give the bridging carbonyl cyclooctenyl derivatives $(OC)_4M(\mu\text{-}PPh_2)(\mu\text{-}CO)Pt(\eta^3\text{-}C_8H_{13})$ (**8a,c**) (eq 8). The molecular structure of **8a,c** has

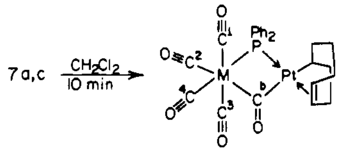

8a,c

(8)

been determined by IR and NMR spectroscopy (Table IV) and by a single-crystal X-ray diffraction study of **8a** (see below and Figure 2). In the IR spectra ν(CO) absorptions typical of a cis-$(OC)_4M$ moiety together with an absorption at 1831 cm^{-1} (**8a**) or 1857 cm^{-1} (**8b**), assignable to a semibridging carbonyl (see discussion of structure), are observed. The ^{31}P{^{1}H} NMR spectrum of **8a** exhibits a 1:4:1 triplet at δ 114 ppm ($^1J_{^{195}Pt\text{-}^{31}P_\mu}$ 3151 Hz) assignable to the μ-PPh_2 ligand. The value of $J_{^{195}Pt\text{-}^{31}P_\mu}$ for **8** is larger than that for the terminal hydride **2c** (1530 Hz) and those for the bridged hydrides **3** (ca. 1500 Hz) consistent with the lower trans influence of the trans olefinic ligand.[32] The ^{13}C{^{1}H} NMR

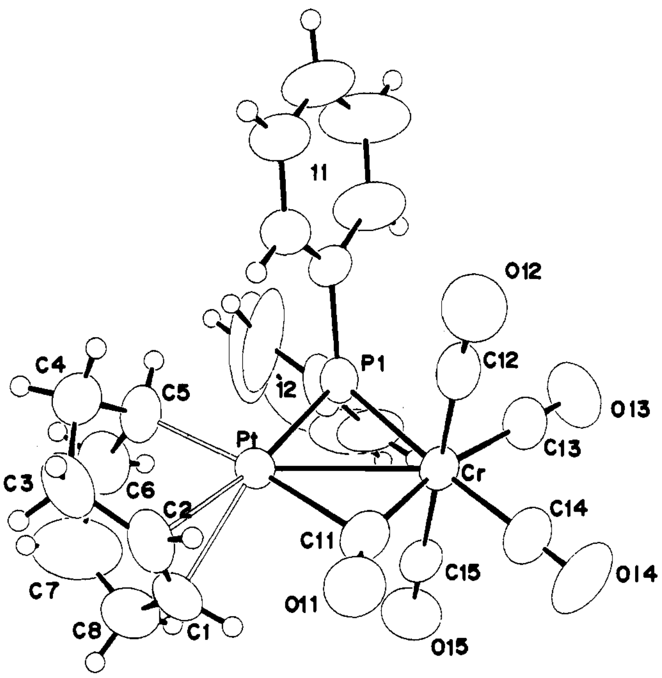

Figure 2. Molecular structure of $(OC)_4Cr(\mu\text{-}PPh_2)(\mu\text{-}CO)Pt(\eta^3\text{-}cyclooctenyl)$ (**8a**) as determined by single-crystal X-ray diffraction. Selected bond lengths (Å): Pt–Cr = 2.820 (1), Pt–P1 = 2.239 (2), Pt–C1 = 2.275 (7), Pt–C2 = 2.272 (7), Pt–C5 = 2.073 (7), Pt–C11 = 2.252 (7), Cr–P1 = 2.342 (2), Cr–C11 = 1.976 (7). Selected bond angles (deg): Pt–P1–Cr = 75.93 (6), P1–Pt–C5 = 95.2 (2), P1–Pt–C11 = 97.2, C5–Pt–C11 = 164.9 (3), P1–Cr–C11 = 102.2 (2).

spectrum of the cyclooctenyl ligand (Table IV) includes a resonance at ca. 34 ppm, $J_{^{195}Pt\text{-}^{13}C}$ = ca. 700 Hz, assignable to the η^1-C atom, together with two resonances in the range 110–120 ppm with $J_{^{195}Pt\text{-}^{13}C}$'s in the range 60–90 Hz, assignable to η^2-olefinic carbon atoms. The considerably lower value of $J_{^{195}Pt\text{-}olefinic^{13}C}$ in the η^1-cyclooctenyl complex **8** compared to the values of ca. 240 Hz observed for $[(\eta^3\text{-}2\text{-methoxycyclooctenyl})PtCl(py)]$[33] is consistent with the larger trans influence of phosphine ligands. The

---

(32) Appleton, T. G.; Clark, H. C.; Manzer, L. E. *Coord. Chem. Rev.* **1973**, *10*, 335.

(33) Powell, J.; Cooper, D. G. *Inorg. Chem.* **1977**, *16*, 142.

Scheme II. Possible Mechanisms for the Intramolecular Bridge ⇌ Terminal CO Exchange Process in **8a,c**[a]

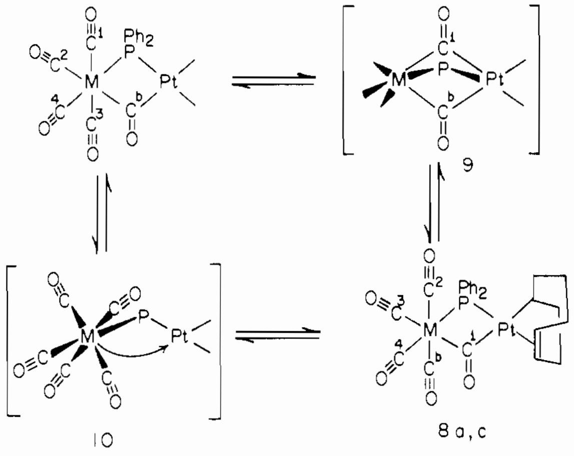

[a] Evidence suggests that the route via intermediate **10** is the more probable.

^{13}C NMR studies of **8** indicate a rapid exchange between the bridging-CO and the terminal-carbonyl ligand 1, 2, and 3, while the C^4 carbonyl trans to the μ-PPh$_2$ remains unique (see Table IV for fast-exchange-limit data, 20 °C). A mechanism involving the associative formation of a second μ-CO group by one of the axial carbonyls, intermediate **9** (Scheme II), could account for this observation. An alternative, *and very likely more probable mechanism*, would involve formation of the "all-terminal"-carbonyl species **10** with a dative M → Pt bond. The proposed intermediate **10** is very similar to the structures reported for (OC)$_4$(PMe$_3$)Cr(μ-P^{t}Bu$_2$)NiCl(PMe$_3$)[34] and (OC)$_4$(PMe$_3$)W{C(OMe)Ph}Pt(PMe$_3$)$_2$.[35] A similar exchange between a "semibridging CO" and terminal CO has been observed in Cp(OC)Mo(μ-PPh$_2$)(μ-CO)Pt(PPh$_3$)$_2$.[36] The complexes **8a,c** react reversibly with CO (1 atm) in CH$_2$Cl$_2$ solution to give a complex formulated as (OC)$_5$M(μ-PPh$_2$)Pt(CO)(η^3-cyclooctenyl) (**11**), based on its IR ν(CO) region (see Experimental Section). On removal of CO, **8a,c** are rapidly regenerated.

Addition of a molar equivalent of PPh$_3$ to a CD$_2$Cl$_2$ solution of the μ-carbonyl cyclooctenyl complex **8a** gives the μ-hydrido terminal-carbonyl complex (OC)$_4$Cr(μ-PPh$_2$)(μ-H)Pt(CO)(PPh$_3$) (**6g**) as the major product together with smaller amounts of the μ-hydride (OC)$_4$Cr(μ-PPh$_2$)(μ-H)Pt(PPh$_3$)$_2$ (**3a**) and a third hydride species formulated as (OC)$_5$Cr(μ-PPh$_2$)PtH(CO)(PPh$_3$) (**12**) (eq 9). Addition of a second equivalent of PPh$_3$ converts **6g** and **12** to **3a** (**12** via **2a**). The structural assignments of **6a** and **12** are based primarily on their ^{1}H NMR spectra (Table III). The hydridic resonance of **12** consists of a 1:4:1 triplet of doublets of doublets (δ 12.4 and $J_{^{31}P-^1H}$ = 18.4 Hz) with a $J_{^{195}Pt-^1H}$ of 971 Hz, very similar to the corresponding data for the isolable complex (OC)$_4$Fe(μ-PPh$_2$)PtH(CO)(PCy$_3$) ($J_{^{31}P-^1H}$ = 13.3, 16.5 Hz; $J_{^{195}Pt-^1H}$ = 980 Hz).[37]

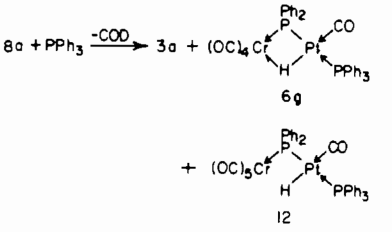

(9)

Reaction of *cis*-M(CO)$_4$(PEt$_3$)(PPh$_2$H) with Pt(C$_2$H$_4$)$_2$(PCy$_3$). The mixed tertiary-phosphine–secondary-phosphine complexes *cis*-M(CO)$_4$(PEt$_3$)(PPh$_2$H)(M = Mo, (**13a**), W (**13b**)) were prepared in ca. 70% yield by following the procedure outlined in eq 10.[24] In CH$_2$Cl$_2$ solution, the complexes **13a,b** oxidatively add to Pt(C$_2$H$_4$)$_2$(PCy$_3$) to give the μ-carbonyl terminal hydride complexes (OC)$_3$(PEt$_3$)M(μ-PPh$_2$)(μ-CO)PtH(PCy$_3$) (**14a,b**) (eq 11). The reaction is rather slow (>90% complete in ca. 24 h at room temperature), and no intermediate species are observed. This suggests that the initial oxidative addition of the P–H bond is the slow step and the considerably reduced rate, in comparison to the formation of (OC)$_4$M(μ-PPh$_2$)(μ-H)Pt(CO)(PCy$_3$) (**6a–c**) (eq 5—reaction complete in ca. 15 min), is probably a consequence of the weaker acidity of the P–H bond in *cis*-M(CO)$_4$(PEt$_3$)(PPh$_2$H) vis-à-vis M(CO)$_5$(PPh$_2$H), though steric effects may also contribute to the slower rate.

$$\mathrm{Et_4N[M(CO)_4(PEt_3)Cl] + PPh_2H \xrightarrow{EtOH} \mathit{c}is\text{-}M(CO)4(PEt_3)(PPh_2H)} \quad (10)$$

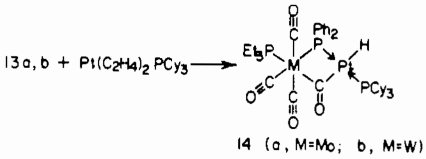

(11)

The structure of **14** is readily established by elemental analysis and IR and ^{1}H, ^{13}C, and ^{31}P{^{1}H} NMR spectroscopy (Table V). The IR (ν(CO) region) spectrum exhibits two absorptions at ca. 2005 (m) and ca. 1900 cm^{-1} (s, br) with relative intensities typical of a *mer*-M(CO)$_3$ arrangement, together with an absorption at ca. 1740 cm^{-1} assignable to a bridging CO. (The lower value of the bridging ν(CO) vis-â-vis that of **8a** suggests a more symmetrical μ-CO structure.) The ^{13}C{^{1}H} NMR spectrum (carbonyl region) contains a 1:4:1 triplet of 1:1:1:1 quartets [δ 246 (M = Mo), $J_{^{195}Pt-^{13}C}$ – 250 Hz, $J_{^{31}P-cis-^{13}C} \simeq$ 0 and 6 Hz, $J_{^{31}P-trans-^{13}C}$ = 24 Hz] assignable to the bridging carbonyl. The observed $J_{^{195}Pt-^{13}C_\mu}$ of ca. 250 Hz for the bridging carbonyl is considerably larger than that reported for the "semibridging CO" in CpMo(CO)$_2$(μ-PPh$_2$)Pt(PPh$_3$)$_2$ (56 Hz),[36] suggesting a stronger OCμ–Pt σ-bonding interaction in **14**. A 1:2:1 triplet (δ 209, $J_{^{31}P-^{13}C}$ = 10 Hz) is assignable to the axial CO's of **14a**, and a 1:1:1:1 quartet (δ 217, $J_{^{31}P-^{13}C}$ = 1.8 and 10 Hz) is assignable to CO trans to μ-PPh$_2$. The disposition of the μ-PPh$_2$ ligand trans to PCy$_3$ on Pt and cis to PEt$_3$ on M is confirmed by the ^{31}P{^{1}H} NMR data where a typical trans $J_{^{31}P_\mu-^{31}P_{Cy_3}}$ (ca. 200 Hz) and a cis $J_{^{31}P-^{31}P_{Et_3}}$ (ca. 26 Hz) are observed. The magnitude of the cis coupling is comparable to the cis $J_{^{31}P-^{31}P(W)}$ of 27.7 Hz reported for *cis*-(OC)$_4$(PPh$_3$)W(μ-PPh$_2$)Ir(CO)$_2$(PPh$_3$).[38] [The corresponding trans isomer of this compound exhibited a $J_{^{31}P_\mu-^{31}P_{(W)}}$ of 58.3 Hz]. The hydrido ligand in **14** exhibits two cis $J_{^{31}P-^1H}$ coupling constants of 6 and 24 Hz and a large $J_{^{195}Pt-^1H}$ value of ca. 1250 Hz typical of a terminal hydride.

In CD$_2$Cl$_2$ the complex (OC)$_3$(PEt$_3$)Mo(μ-PPh$_2$)(μ-CO)PtH(PCy$_3$) (**14a**) equilibrates with the corresponding μ-hydrido terminal-carbonyl isomer (OC)$_3$(PEt$_3$)Mo(μ-PPh$_2$)(μ-H)Pt(CO)(PCy$_3$) (**15a**) (eq 12). At 25 °C the **14a**:**15a** ratio is ca. 5:1 while in C$_6$D$_6$ solution only the μ-carbonyl species **14a** is observed. The structure of **15a** is readily confirmed by ^{1}H and ^{31}P{^{1}H} NMR spectroscopy (Table V).

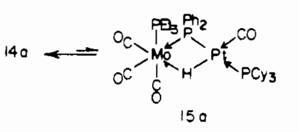

(12)

The formation of **14a,b** with PEt$_3$ trans to the μ-CO can be rationalized on the basis that in the initially formed proposed intermediate **16** (eq 13) it is the CO trans to PEt$_3$ that will be

---

(34) Jones, R. A.; Lasch, J. G.; Norman, N. C.; Stuart, A. L.; Wright, T. C.; Whittlesey, B. R. *Organometallics* **1984**, *3*, 114.

(35) Howard, J. A. K.; Mead, K. A.; Moss, J. R.; Navarro, R.; Stone, F. G. A.; Woodward, P. *J. Chem. Soc., Dalton Trans.* **1981**, 743.

(36) Farrugia, L. J.; Miles, A. D.; Stone, F. G. A. *J. Chem. Soc., Dalton Trans.* **1984**, 2415.

(37) Powell, J.; Gregg, M. R. Unpublished results.

(38) Breen, M. J.; Shulman, P. M.; Geoffroy, G. L.; Rheingold, A. L.; Fultz, W. C. *Organometallics* **1984**, *3*, 782.

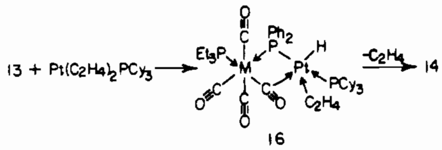

16

(13)

the most nucleophilic with respect to displacement of C_2H_4 from the platinum. The rearrangement at Mo from a *mer* to a *fac* arrangement of carbonyls on going from **14a** to **15a** (eq 12) may be a mechanistic consequence, though the exact nature of this isomerization process is not readily apparent. In contrast to the molybdenum system (eq 12), the tungsten complex **14b** does not equilibrate to a detectable extent with a μ-hydrido analogue.

Although not studied in as much detail as the above triethylphosphine systems, the complexes *cis*-$M(CO)_4(PR_3)(PPh_2H)$ (PR_3 = $PMePh_2$, PPh_3) likewise react with $Pt(C_2H_4)_2(PCy_3)$ in CH_2Cl_2 to give complexes that have IR (ν(CO)) and ^1H and $^{31}P\{^1H\}$ NMR spectra consistent with their being structural analogues of **14**. However, the reaction with *cis*-$M(CO)_4(PPh_3)(PPh_2H)$ takes several days at room temperature, and several side reactions are observed to occur within this time scale.

Molecular Structure of $(OC)_4Cr(\mu\text{-}PPh_2)(\mu\text{-}H)Pt(PEt_3)_2$ (3d). An ORTEP drawing of **3d** giving the atom-labeling scheme is shown in Figure 1. The geometry at platinum is essentially planar and very similar to that reported for $[PtH(PEt_3)_3]PF_6$[39] and $[PtH(PPh_3)_3][(CF_3CO_2)_2H]$,[40] the large ∠PPtP angles between adjacent phosphorous ligands (ca. 101°) being reflective of the large steric requirements of these ligands.[41] While the position of the hydride ligand was not determined, its location at the bridge position is consistent with the observed ^1H NMR data and provides platinum with a four-coordinate planar coordination sphere and chromium with a pseudooctahedral coordination sphere. Formulation of the structure of **3d** with a bent 3c–2e CrHPt bond is also consistent with the structures of $[(\eta^5\text{-}Cp)(ON)Re(\mu\text{-}PR_2)(\mu\text{-}H)Pt(PPh_3)_2]^+$ (R = Cy, Ph) where the hydride ligand was located and shown to occupy a comparable position to that suggested for **3d**.[17] The μ-phosphido ligand exhibits an acute ∠CrPPt of 75°. The CrPt separation of 2.905 (2) Å, while well within the range expected for a CrPt bond, does not necessarily imply a *direct* metal–metal bond. Several studies have concluded that metal–metal bonding in some doubly bridged binuclear systems is better discussed in terms of multicentered linkages between the metals and the bridging groups.[42] Indeed, the structural similarities between **3d** and $[PtH(PEt_3)_3]^+$ [39] suggest rather similar distributions of electron density about the platinum, which might not be the case if there were a significant *direct* CrPt bond in **3d**. Consequently, we suggest that direct CrPt bonding is at best relatively weak with most of the bonding between Cr and Pt occurring via the bridged ligands as signified in **3** (eq 2).

Molecular Structure of $(OC)_4Cr(\mu\text{-}PPh_2)(\mu\text{-}CO)Pt(\eta^3\text{-}cyclooct\text{-}4\text{-}en\text{-}1\text{-}yl)$ (8a). The structure of **8a** consists of an approximately octahedral "$Cr(CO)_5(\mu\text{-}PPh_2)$" unit bonded to a "$Pt(\eta^3\text{-}cyclooctenyl)$" moiety via a bridging-$PPh_2$ and a semibridging-carbonyl ligand (Figure 2). The essentially planar stereochemistry at Pt (excluding the possibility of a direct Cr–Pt interaction) is similar to the mononuclear complex $PtCl(py)(\eta^3\text{-}2\text{-}methoxycyclooct\text{-}4\text{-}en\text{-}1\text{-}yl)$.[43] The "$\mu$-$PPh_2$, semibridging-CO" unit is very similar to the comparable bonding arrangement in $(OC)_3(PMe_3)Cr(\mu\text{-}P^tBu_2)(\mu\text{-}CO)Rh(CO)(PMe_3)$ (**17**).[34] The Cr–C(11)–O(11) angle of 151.8 (6)° and the C(11)Pt distance of 2.252 (7) Å in **8a** are 159.6 (5)° and 2.259 (6) Å (C–Rh) in **17**. In $[(\eta^5\text{-}Cp)(OC)Mn(\mu\text{-}C\text{-}tolyl)(\mu\text{-}CO)Pt(PMe_3)_2]BF_4$ (**18**) the corresponding values are 157.5 (9)° and 2.31 (1) Å.[44] Again the question of whether or not the CrPt distance of 2.820 (1) Å in **8a** implies a significant *direct* CrPt bond is open to debate as discussed above.[42] Although the Pt–C(semibridging CO) bond is rather long, it is still within a reasonable bonding distance given the average value of 2.274 (7) Å for the Pt–C(olefinic carbons) of the enyl ligand. Consequently, we suggest in this system also that most of the chromium–platinum bonding occurs via the bridging ligands. One of several possible representations of the bonding is the Cr(II)–Pt(II) formulation given in **8a,c** (eq 8). The higher ν(CO) values of **8a,c**, vis-à-vis **3a,c**, for which a Cr(0)–Pt(II) formulation has been suggested, are consistent with reduced electron density on Cr.

In discussing the semibridging-carbonyl ligand in $(OC)_3(PMe_3)Cr\{\mu\text{-}CPh(CO_2Me)\}(\mu\text{-}CO)Pt(PMe_3)_2$ (**19**) and $[Cp(OC)Mn(\mu\text{-}C\text{-}tolyl)(\mu\text{-}CO)Pt(PMe_3)_2]BF_4$ (**18**), Stone et al.[44] have chosen to describe the bonding in terms of electron donation from the platinum to the π^* orbital of the carbonyl ligand. Such a description requires the Pt to be considered in terms of a Pt(0) formulation. In **8a**, the presence of the cyclooctenyl ligand and the similarity of the geometry at Pt relative to $PtCl(py)(2\text{-}methoxycyclooctenyl)$[43] suggest that a Pt(II) formulation is more appropriate. Furthermore, the high ν(CO) stretching frequencies for the terminal-carbonyl ligand on Pt in the complexes $(OC)_5Cr(\mu\text{-}PPh_2)Pt(CO)(\eta^3\text{-}cyclooctenyl)$ (**11**; 2074 cm^{-1}), and $(OC)_4M(\mu\text{-}PR_2)(\mu\text{-}H)Pt(CO)(PCy_3)$ (**6**; 2062–2070 cm^{-1}) are indicative of only weak Pt to π^* CO π-bonding. An alternative and perhaps more appropriate description of the bonding of the semibridging carbonyl in **8a** (and structurally similar systems) would consider the Pt(μ-CO) bond to be similar to an acyl–Pt bond with the added proviso that the MC(O)–Pt bond is more easily polarized than the RC(O)–Pt analogue. In this regard, one would expect considerable variation in Pt–C(μ-CO) bond lengths as a consequence of the varying trans influence of the trans ligand [large for "yl" (**8a**) and PMe_3 (**18** and **19**)]. In this respect, the bridging-CO ligand could be regarded as being similar to, though even more polarizable than, Pt–Cl bonds.[32] [Long Pt–C bonds of 2.56 (9) Å have also been observed in $[Pt(CH_3)_3(acac)]_2$ between Pt and the γ-C of the acac ligand,[45] an unusual complex in which the bridging-acac ligand can likewise be considered to be easily polarized.] Other μ-phosphido-bridged complexes in which significant direct metal–metal bonding *can* be considered to occur include systems containing singly bridging μ-PR_2 ligands and no other bridging groups such as $(OC)_4(PMe_3)Cr(\mu\text{-}P^tBu_2)NiCl(PMe_3)$,[34] $(OC)_3(PPh_3)Fe(\mu\text{-}PPh_2)Ir(CO)_2(PPh_3)$,[46] $(OC)_5W(\mu\text{-}PPh_2)Re(CO)_4$[4], $[Cp(ON)HRe(\mu\text{-}PCy_2)Pt(PPh_3)_2]^+$,[17] and $Cp(OC)_2W(\mu\text{-}PPh_2)Pt(CO)(PPh_3)$.[16] In these systems the observed stereochemical features of the molecules can best be rationalized by assuming a "bent" MM′ bond with the coordination at Ni/Pt being essentially planar and very similar to that of mononuclear Ni/Pt analogues.

Discussion

The relative rate of formation of **2a–c** from the oxidative addition of **1a–c** to $Pt(C_2H_4)(PPh_3)_2$ (eq 2) parallels the observed acidity of the P–H bond observed for $(OC)_5M(PH_3)$ as a function of M.[25] The marked decrease in reactivity with respect to oxidative addition processes on going from $M(CO)_5(PPh_2H)$ to $M(CO)_5(PR_2H)$ (R = Cy or *n*-Pr), or to $M(CO)_4(PR_3)(PPh_2H)$ are consistent with the relative acidity of the P–H bond being a significant factor in determining the ease of oxidative addition

---

(39) Russell, D. R.; Mazid, M. A.; Tucker, P. A. *J. Chem. Soc., Dalton Trans.* **1980**, 1737.

(40) Caputo, R. E.; Mak, D. K.; Willett, R. D.; Roundhill, S. G. N.; Roundhill, D. M. *Acta Crystallogr.* **1977**, *B33*, 215.

(41) Clark, H. C.; Hampden-Smith, M. J. *Coord. Chem. Rev.* **1987**, *79*, 229.

(42) (a) Benard, M.; Dedieu, A.; Nakamura, S. *Nouv. J. Chim.* **1984**, *8*, 149. (b) Jemmis, E. D.; Pinhas, A. R.; Hoffmann, R. *J. Am. Chem. Soc.* **1980**, *102*, 2576. (c) Benard, M. *J. Am. Chem. Soc.* **1978**, *100*, 7740. (d) Benard, M. *Inorg. Chem.* **1979**, *18*, 2782. (e) Mason, R.; Mingos, D. M. P. *J. Organomet. Chem.* **1973**, *50*, 53. (f) Summerville, R. H.; Hoffmann, R. *J. Am. Chem. Soc.* **1976**, *98*, 7240. (g) Lauher, J. W.; Elian, M.; Summerville, R. H.; Hoffmann, R. *J. Am. Chem. Soc.* **1976**, *98*, 3219. (h) Churchill, M. R.; DeBoer, B. G.; Rotella, F. T. *Inorg. Chem.* **1976**, *15*, 1843.

(43) Bombieri, G.; Forsellini, E.; Greziani, R. *J. Chem. Soc., Dalton Trans.* **1972**, 525.

(44) Howard, J. A. K.; Jeffery, J. C.; Laguna, M.; Navarro, R.; Stone, F. G. A. *J. Chem. Soc., Dalton Trans.* **1981**, 751.

(45) Hazell, A. C.; Truter, M. R. *Proc. R. Soc. London* **1960**, *A254*, 218.

(46) Roberts, D. A.; Steinmetz, G. R.; Breen, M. J.; Shulman, P. M.; Geoffroy, G. L. *Organometallics* **1983**, *2*, 846.

Scheme III. Possible Reaction Pathways for the Formation of $(CO)_4M(\mu\text{-}PPh_2)(\mu\text{-}H)Pt(PPh_3)_2$ (**3**) from $(OC)_5M(\mu\text{-}PR_2)PtH(PPh_3)_2$ (**2**) [Obtained from $(OC)_5M(PR_2H)$ (**1**) and $Pt(C_2H_4)(PPh_3)_2$]^a

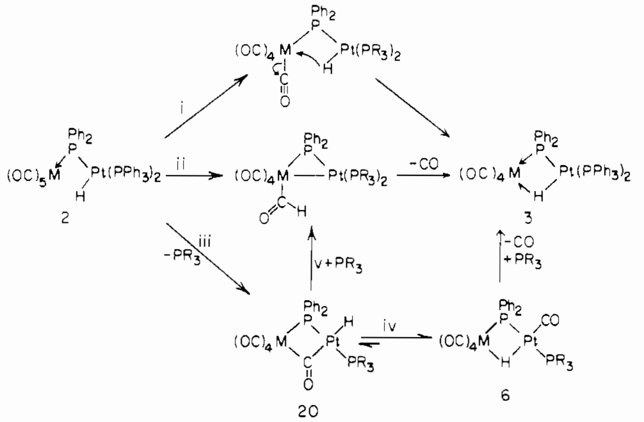

^{a}The data support route iii → iv as the preferred reaction pathway.

although steric factors are also likely to contribute to the difference in rates. This and other studies involving the reactions of $[Cp(OC)_3W(PPh_2H)]^+$[16] and $[Cp(ON)(OC)Re(PR_2H)]^+$[17] to zerovalent platinum complexes are consistent with an initial protonation of the platinum to give $[PtH(C_2H_4)(PPh_3)_2]^+$ followed by rapid reaction with the resultant $[M]PPh_2$ ligand as being the probable mechanism for the formation of **2**. Possible mechanisms for loss of CO from **2** and formation of the bridging-hydride **3** are illustrated in Scheme III. The remarkable ease of substitution of CO into, or from, the group VI metal center under room-temperature conditions, and the relative rate of the **2** → **3** rearrangement as a function of the group VI metal (Cr > Mo ≫ W) are not typical of the known thermal CO substitution reactions of group VI metal carbonyls, which are typically slow, frequently require high temperatures (100–200 °C), and exhibit relative rates as a function of M in the order Mo ≫ Cr > W.[21] Consequently, a simple ligand substitution process (Scheme III, route i) seems most unlikely. Studies of the relative rates of **2** ⇄ **3** interconversion have shown that CO substitution at M of **2** is very sensitive to the nature of the phosphine ligands on the platinum metal (relative rates for **2** → **3** and **3** → **2**: $PPh_3 \sim PEt_3 \gg$ dppe) provides a strong argument for an "adjacent platinum-assisted mechanism involving PR_3 dissociation". Hydride ligands are known to be good trans labilizers of tertiary-phosphine ligands.[32] Also it should be noted that the addition of the good π-acid ^nBuNC to **2** or **3** rapidly displaces the PPh_3 ligand trans to the hydride ligand and likewise inhibits CO addition/displacement from the group VI metal. On the basis of these observations, a mechanism involving the formation of a formyl intermediate via direct hydride attack on a coordinated CO (Scheme III, route ii, no PR_3 dissociation) can be excluded. The involvement of a μ-CO intermediate, **20**, and a μ-hydrido terminal-carbonyl, **6** (Scheme III, routes iii and iv), is consistent with the effect of phosphines on the rate (i.e. displacement of dppe is more difficult than loss of PR_3 ligands). The complexes **8a**,**c** (see Figure 2) and **14** are close models of the μ-carbonyl intermediate **20**, and the equilibrium **14a**–**15a** (eq 12) closely models the rearrangement of **20** to the μ-hydrido terminal-carbonyl **6** (the PPh_3 analogue of the complexes **6a**–**f**). The formation of **6g** and **3a** on addition of PPh_3 to **8a** (eq 9) lends further support to the **20** → **6** rearrangement. Addition of PPh_3 to **6** and displacement of CO from the platinum leads to the bridging-hydrido complexes **3**. It should be noted that addition of PPh_3 to **6** also leads to some regeneration of **2** (e.g., see eq 6) and that the relative rates of **6** → **3** and **6** → **2** as a function of M probably contributes in part to the relative rate of the **2** → **3** rearrangement (eq 2; Cr > Mo > W). Further support for route iii → iv, Scheme III, as the mechanism of CO loss from **2** is obtained from the reaction of $Cr(CO)_5(PPh_2H)$ with a large excess of $Pt(C_2H_4)(PPh_3)_2$. Under these conditions, two hydridic intermediate species are observed. One is a broad resonance at δ −10.5 with $J_{^{195}Pt-^1H}$ of ca. 700 Hz that is assigned to $(OC)_4Cr(\mu\text{-}PPh_2)(\mu\text{-}H)Pt(CO)(PPh_3)$ (**6q**) (see Table III for data for **6q** prepared in situ from the addition of PPh_3 to **8a**). The broadness of this resonance in the presence of excess $Pt(C_2H_4)(PPh_3)_2$ may be a consequence of PPh_3 exchange. The initial formation of **6g** from **2a** is probably encouraged by the presence of $Pt(C_2H_4)(PPh_3)_2$, which functions as a PPh_3 scavenger (eq 14). The other intermediate hydridic species is also broad

Scheme IV. Postulated Steps for the Formation of $(OC)_4M(\mu\text{-}PR_2)(\mu\text{-}H)Pt(CO)(PCy_3)$ (**6**)

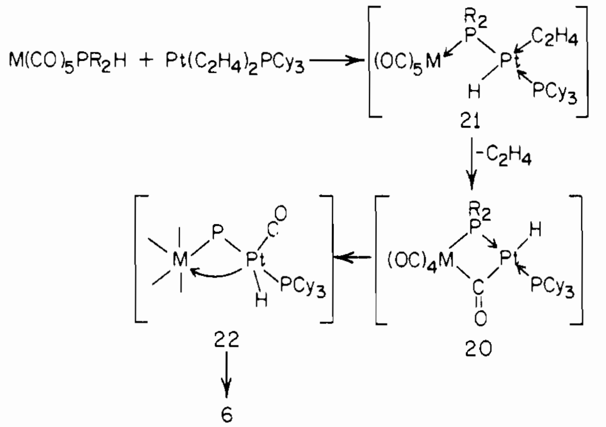

$$\mathbf{2a} + 2Pt(C_2H_4)(PPh_3)_2 \rightarrow \mathbf{6g} + Pt(PPh_3)_3 + 2C_2H_4 \qquad (14)$$

($\Delta\nu_{1/2} \sim 25$ Hz) with $J_{^{195}Pt-^1H} \simeq 780$ Hz. The identity of this species is not readily apparent. Established $J_{^{195}Pt-^1H}$ values for "$Cr(\mu\text{-}PPh_2)Pt$" hydrido species are 853 Hz for $(OC)_5Cr(\mu\text{-}PPh_2)PtH(PPh_3)_2$ (**2a**), 648 Hz for $(OC)_4Cr(\mu\text{-}PPh_2)(\mu\text{-}H)Pt(PPh_3)_2$ (**3a**), 697 Hz for $(OC)_4Cr(\mu\text{-}PPh_2)(\mu\text{-}H)Pt(CO)(PPh_3)$ (**6g**), and 971 Hz for $(OC)_5Cr(\mu\text{-}PPh_2)PtH(CO)(PPh_3)$ (**12**). A possibility for this intermediate is an ethylene complex $(CO)_4Cr(\mu\text{-}PPh_2)(\mu\text{-}H)Pt(C_2H_4)(PPh_3)$, structurally similar to **6g**, but this must be regarded as tentative.

Finally, the possibility of a mechanism involving a formyl intermediate, formed via reductive coupling of μ-CO and H (i.e. route iii → v, Scheme III) can be excluded on the grounds that such a process is unlikely to be readily reversible in contrast to the ease with which **2** is re-formed from **3** and CO.

Following a preliminary account of these studies, Schwald and Peringer[47] reported that the reaction of the primary phosphine complexes $(OC)_5M(PPhH_2)$ (M = Cr, Mo, W) with $Pt(C_2H_4)(PPh_3)_2$ leads to the single-bridge μ-phosphido complex $(OC)_5M(\mu\text{-}PPhH)PtH(PPh_3)_2$, structurally similar to the $\mu\text{-}PPh_2$ complexes **2**. In contrast to **2** (eq 2), $(OC)_5M(\mu\text{-}PPhH)PtH(PPh_3)_2$ does *not* readily lose CO and may be recrystallized from solution without CO loss. *This observation clearly indicates that the platinum-assisted CO loss process is very sensitive to the nature of the bridging ligand.* A plausible explanation invokes the Thorp–Ingold effect[48] whereby bulky *gem* substituents on the μ-P atom of **2** promote the formation of a four-atom ring (i.e., formation of **20**, Scheme III, route iii). A similar proposal has been put forward to account for the sensitivity of orthometalation reactions of "$PPhR_2$ complexes" and similar systems to the size (steric bulk) of the R groups.[49]

In view of the results obtained from the reaction of $M(CO)_5(PPh_2H)$ with $Pt(COD)_2/C_2H_4$ (see above, eq 7 and 8) a likely mechanism for the formation of **6a**–**f** is shown in Scheme IV. Oxidative addition of the P–H bond of **1** across the platinum gives the terminal hydrido platinum derivative **21**, which is not observed but is structurally analogous to $(OC)_5M(\mu\text{-}PPh_2)PtH(L)_2$ [$(L)_2$ = COD, (**7**), $(PPh_3)_2$ (**2a**–**c**), $(CO)(PPh_3)$, (**6g**)]. Loss of

---

(47) Schwald, J.; Peringer, P. *J. Organomet. Chem.* **1987**, *323*, C51.

(48) Eliel, E. L.; Allinger, N. L.; Angyal, S. J.; Morrison, G. A., *Conformational Analysis*; Interscience: New York, 1965; p 191.

(49) Shaw, B. L. *J. Am. Chem. Soc.* **1975**, *97*, 3856.

(50) Powell, J.; Sawyer, J. F.; Stainer, M. V. R. Manuscript in preparation.

Table VI. Positional Parameters and Their Estimated Standard Deviations

atom	*x*	*y*	*z*	*B*,[a] Å^2	atom	*x*	*y*	*z*	*B*,[a] Å^2
(a) (OC)$_4$Cr(μ-PPh$_2$)(μ-H)Pt(PEt$_3$)$_2$ (**3d**)									
Pt	0.000	0.02940 (2)	0.000	2.435 (4)	C21	−0.027 (1)	0.289 (1)	0.0795 (8)	7.1 (4)
Cr	0.17821 (9)	0.0167 (1)	0.11945 (8)	2.93 (3)	C22	−0.084 (1)	0.228 (2)	0.1139 (9)	10.8 (5)
P1	−0.1261 (2)	−0.0512 (2)	−0.0904 (1)	3.11 (5)	C23	0.0522 (8)	0.304 (1)	−0.0329 (8)	5.8 (3)
P2	−0.0334 (2)	0.2269 (2)	−0.0152 (2)	3.51 (5)	C24	0.0593 (9)	0.267 (2)	−0.1106 (8)	8.2 (4)
P3	0.0901 (1)	−0.1325 (2)	0.0435 (1)	2.59 (4)	C25	−0.1349 (8)	0.2825 (9)	−0.0938 (9)	6.1 (4)
O1	0.1207 (6)	−0.0488 (7)	0.2500 (5)	5.3 (2)	C26	−0.141 (1)	0.416 (1)	−0.101 (1)	7.3 (4)
O2	0.2344 (7)	0.2507 (8)	0.1962 (5)	7.1 (3)	C311	0.0590 (6)	−0.2455 (7)	0.0964 (5)	3.1 (2)
O3	0.2629 (6)	0.091 (1)	0.0100 (5)	8.5 (3)	C312	−0.0153 (6)	−0.2318 (9)	0.1139 (5)	3.9 (2)
O4	0.3504 (6)	−0.088 (1)	0.2194 (6)	7.8 (3)	C313	−0.0369 (7)	−0.320 (1)	0.1558 (6)	5.1 (3)
C1	0.1421 (6)	−0.0215 (8)	0.2014 (5)	3.2 (2)	C314	0.0142 (8)	−0.416 (1)	0.1838 (6)	5.2 (3)
C2	0.2112 (7)	0.1593 (9)	0.1653 (6)	4.2 (2)	C315	0.0907 (8)	−0.429 (1)	0.1689 (7)	5.1 (3)
C3	0.2276 (7)	0.060 (1)	0.0484 (6)	4.7 (2)	C316	0.1122 (7)	−0.3442 (9)	0.1233 (6)	4.2 (2)
C4	0.2823 (7)	−0.051 (1)	0.1795 (6)	4.5 (2)	C321	0.0975 (5)	−0.2109 (7)	−0.0410 (5)	2.7 (2)
C11	−0.2223 (7)	−0.009 (1)	−0.0726 (8)	4.8 (3)	C322	0.0697 (6)	−0.3270 (7)	−0.0603 (5)	3.3 (2)
C12	−0.2198 (8)	−0.054 (1)	0.0094 (8)	6.4 (3)	C323	0.0710 (7)	−0.3773 (8)	−0.1293 (6)	4.3 (2)
C13	−0.158 (1)	0.002 (1)	−0.1896 (7)	6.5 (4)	C324	0.1020 (7)	−0.3179 (9)	−0.1765 (5)	4.2 (2)
C14	−0.084 (1)	−0.021 (2)	−0.2240 (9)	8.9 (5)	C325	0.1321 (7)	−0.2043 (9)	−0.1574 (5)	4.4 (2)
C15	−0.1313 (7)	−0.2085 (9)	−0.0990 (7)	4.4 (2)	C326	0.1295 (7)	−0.1525 (8)	−0.0903 (6)	4.0 (2)
C16	−0.2186 (8)	−0.263 (1)	−0.1531 (8)	5.3 (3)					
Compound **8a**									
Pt	0.12550 (1)	−0.00419 (3)	0.23866 (2)	3.159 (4)	C12	0.1089 (3)	−0.1659 (8)	−0.0846 (7)	4.4 (2)
Cr	0.16777 (5)	−0.1748 (1)	0.0360 (1)	3.37 (2)	C13	0.1731 (3)	−0.3552 (8)	−0.0009 (8)	4.9 (2)
P1	0.10670 (8)	−0.2180 (2)	0.2132 (2)	3.39 (4)	C14	0.2122 (3)	−0.1424 (8)	−0.1140 (8)	4.8 (2)
O11	0.1875 (3)	0.1180 (5)	−0.0019 (6)	6.4 (2)	C15	0.2277 (3)	−0.1829 (7)	0.1587 (7)	3.9 (2)
O12	0.0736 (3)	−0.1649 (7)	−0.1609 (5)	7.4 (2)	C111	0.0383 (3)	−0.2547 (7)	0.1716 (7)	3.7 (2)
O13	0.1752 (3)	−0.4665 (6)	−0.0222 (7)	7.4 (2)	C112	0.0032 (3)	−0.1574 (7)	0.1357 (8)	4.5 (2)
O14	0.2378 (3)	−0.1166 (7)	−0.2078 (6)	7.6 (2)	C113	−0.0499 (4)	−0.1858 (9)	0.0984 (9)	5.9 (2)
O15	0.2638 (2)	−0.1848 (6)	0.2290 (6)	6.3 (2)	C114	−0.0670 (4)	−0.308 (1)	0.099 (1)	7.3 (3)
C1	0.1737 (3)	0.1673 (8)	0.3236 (9)	5.6 (2)	C115	−0.0335 (4)	−0.4076 (9)	0.128 (1)	9.8 (3)
C2	0.1283 (4)	0.2183 (7)	0.2620 (8)	5.6 (2)	C116	0.0187 (4)	−0.3824 (8)	0.166 (1)	7.3 (3)
C3	0.0801 (4)	0.2646 (8)	0.330 (1)	6.8 (2)	C121	0.1205 (4)	−0.3234 (7)	0.3647 (7	4.9 (2)
C4	0.0437 (4)	0.1497 (9)	0.377 (1)	6.6 (2)	C122	0.0836 (5)	−0.3333 (9)	0.4683 (9)	10.9 (3)
C5	0.0749 (4)	0.0248 (7)	0.4054 (8)	5.2 (2)	C123	0.0944 (6)	−0.407 (1)	0.5851 (9)	13.1 (4)
C6	0.1021 (4)	0.022 (1)	0.5458 (9)	7.4 (3)	C124	0.1409 (6)	−0.4748 (9)	0.599 (1)	10.5 (4)
C7	0.1420 (5)	0.121 (2)	0.572 (1)	11.6 (4)	C125	0.1752 (4)	−0.4709 (9)	0.494 (1)	9.0 (3)
C8	0.1848 (4)	0.147 (1)	0.476 (1)	7.8 (3)	C126	0.1667 (4)	−0.3970 (9)	0.374 (1)	6.2 (2)
C11	0.1739 (3)	0.0187 (7)	0.0437 (8)	4.5 (2)					

[a] Values for anisotropically refined atoms are given in the form of the isotropic equivalent thermal parameter defined as: $(4/3)[a^2B(1,1) + b^2B(2,2) + c^2B(3,3) + ab(\cos\gamma)B(1,2) + ac(\cos\beta)B(1,3) + bc(\cos\alpha)B(2,3)]$.

ethylene gives the μ-carbonyl species (also not observed but structurally similar to **8**), which then undergoes an intramolecular reorganization, possibly via an intermediate such as **22**, to give the μ-hydrido complexes **6**.

Formation of (OC)$_4$M(μ-PPh$_2$)(μ-H)Pt(PR$_3$)$_2$ from the Reaction of M(CO)$_4$(PPh$_3$)(PPh$_2$Li) with *trans*-PtHCl(PR$_3$)$_2$. Oxidative addition of M(CO)$_4$(PPh$_3$)(PPh$_2$H) to Pt(C$_2$H$_4$)(PPh$_3$)$_2$ (CH$_2$Cl$_2$, room temperature) occurs *very slowly* (days) to give a mixture of products. In contrast, reaction of M(CO)$_4$(PPh$_3$)(PPh$_2$Li) [prepared in situ in THF from the addition of MeLi to M(CO)$_4$(PPh$_3$)(PPh$_2$H)] with *trans*-PtHCl(PR$_3$)$_2$ (PR$_3$ = PEt$_3$, PMe$_2$Ph) occurs reasonably quickly (within minutes at room temperature) to give (OC)$_4$M(μ-PPh$_2$)(μ-H)Pt(PR$_3$)$_2$ (**3e**,**f**,**h**,**i**) isolated in ca 60% yields (eq 15). The formation of **3**

$$cis\text{-M(CO)}_4\text{(PPh}_3\text{)(PPh}_2\text{Li)} + \text{PtHCl(PR}_3\text{)}_2 \rightarrow \mathbf{3} + \text{PPh}_3 + \text{LiCl} \quad (15)$$

in this reaction is somewhat surprising in that it clearly requires a simple and noticeably facile displacement of PPh$_3$ from M in contrast to the CO-transfer mechanism outlined in Scheme III, routes iii + iv, and eq 11 and 12. Indeed it is possible that the formation of **3** from M(CO)$_5$(PPh$_2$Li) and *trans*-PtHCl(PR$_3$)$_2$ (eq 3) may involve direct displacement of CO from M. The reason(s) for the difference in behavior (eq 11, 12 vs eq 15) are not readily apparent.

Experimental Section

General Data. All manipulations were carried out under an atmosphere of dry N$_2$ by using dry, degassed solvents. IR spectra were recorded on a Nicolet 10DX spectrometer. ^{1}H, ^{13}C{^{1}H}, and ^{31}P{^{1}H} NMR spectra were recorded on a Varian XL200 spectrometer and chemical shifts referenced to tetramethylsilane and 85% H$_3$PO$_4$, respectively. Microanalyses were carried out by Canadian Microanalytical Laboratories, Vancouver, B.C., Canada.

Starting Materials. The group VI metal carbonyls and the secondary phosphines PCy$_2$H, PPh$_2$H, and P^{n}Pr$_2$H were purchased from either Pressure Chemical Co. or Strem Chemicals, Inc.; Pt(C$_2$H$_4$)(PPh$_3$)$_2$,[51] Pt(PPh$_3$)$_4$,[52] Pt(COD)$_2$, Pt(C$_2$H$_4$)$_2$PCy$_3$,[53] PtHCl(PEt$_3$)$_2$,[54] PtHCl(PMe$_2$Ph)$_2$,[55] and Et$_4$N[M(CO)$_5$Cl] (M = Cr, Mo, W)[24] were prepared by literature methods. The secondary phosphine complexes M(CO)$_5$(PR$_2$H) (**1**) were prepared from Et$_4$N[M(CO)$_5$Cl] and a stoichiometric amount of PR$_2$H by following the procedure given for the synthesis of M(CO)$_5$(PR$_3$).[24] The complexes M(CO)$_4$(PR$_3$)(PPh$_2$H) (**16**; M = Mo, W; PR$_3$ = PEt$_3$, PMePh$_2$, PPh$_3$) were similarly prepared from the reaction of Et$_4$N[M(CO)$_4$(PR$_3$)Cl] with PPh$_2$H in EtOH.[24]

Preparation of (OC)$_4$W(μ-PPh$_2$)(μ-H)Pt(PPh$_3$)$_2$ (3c). Pt(C$_2$H$_4$)(PPh$_3$)$_2$ (1.00 g, 1.34 mmol) was added to a CH$_2$Cl$_2$ (5 mL) solution of W(CO)$_5$(PPh$_2$H) (0.685 g, 1.34 mmol). The addition of pentanes (15 mL) after 3 h produced a red oil, which on vigorous stirring (10–30 min) turned to a bright yellow solid. The mother liquor was decanted and the solid washed with pentanes (3 × 10 mL) and dried in vacuo to give yellow microcrystalline **3c** in 72% yield. Recrystallization of **3c** from dichloromethane/pentane gave analytically pure material. Complexes **3a** (orange solid, 74% yield) and **3b** (yellow solid, 73% yield) were prepared by following the above procedure. Addition of a molar equivalent of dppe to CH$_2$Cl$_2$ solutions of the complexes **3a–c** gave the corresponding dppe complexes **3j–l** (80% yield) on workup (PPh$_3$ removed by repeated hot hexane washes). (See Table II for analytical and spectroscopic data.)

Preparation of (OC)$_4$W(μ-PPh$_2$)(μ-H)Pt(PEt$_3$)$_2$ (3f). ^{n}BuLi (2.31 M in hexane, 0.34 mL, 0.784 mmol) was added via syringe to a THF (5 mL) solution of W(CO)$_5$(PPh$_2$H) (0.402 g, 0.784 mmol) at 22 °C. After

---

[51] Blake, D. M.; Roundhill, D. M. *Inorg. Synth.* **1978**, *18*, 120.
[52] Ugo, R.; Cariati, F.; LaMonica, G. *Inorg. Synth.* **1968**, *11*, 105.
[53] Spencer, J. L. *Inorg. Synth.* **1979**, *19*, 216.
[54] Parshall, G. W. *Inorg. Synth.* **1969**, *12*, 29.
[55] Clark, H. C.; Kurosawa, H. *Inorg. Chem.* **1972**, *11*, 1276.

the mixture was stirred for a few minutes, *trans*-PtHCl(PEt_3)$_2$ (0.365 g, 0.784 mmol) was added and the solution allowed to stand for 20 h. The resultant yellow crystalline material was filtered, washed with hexane, and dried in vacuo to give **3f** in 44% yield. Complexes **3d,e** and **3g–l** were obtained in ca. 40% yields by following the above procedure.

Preparation of (OC)$_4$Cr(μ-PPh$_2$)(μ-CO)Pt(η^3-cyclooct-4-en-1-yl) (8a). Dry hexane (50 mL) was cooled to 0 °C and saturated with C_2H_4 for 20 min, and Pt(COD)$_2$ (1.26 g, 3.06 mmol) was added in ca. 0.25-g increments. A solution of Cr(CO)$_5$(PPh$_2$H) (1.16 g, 3.06 mmol) in dry hexane (30 mL) was added dropwise to the rapidly stirred solution of "Pt(C_2H_4)$_3$ + COD". The complex (OC)$_5$Cr(μ-PPh$_2$)PtH(COD) (**7a**) rapidly precipitates as a yellow-green solid (ca. 2.0 g, 2.9 mmol, 95% yield). On dissolving in CH_2Cl_2 (room temperature), **7a** isomerizes to **8a** within 10–20 min (100% conversion). Complexes **7c** and **8c** (M = W) were similarly prepared. Isolated yield of **8c**: 30%. Attempts to prepare the molybdenum analogues **7b** and **8b** using the above procedure were not successful and resulted in considerable decomposition. When CO was bubbled through a CH_2Cl_2 solution of **8a** and the reaction followed by IR spectroscopy, new ν(CO) bands at 2074 (m), 2051 (w), and 1927 (s br) cm^{-1} were observed. These are assigned to the in situ formation of (OC)$_5$Cr(μ-PPh$_2$)Pt(CO)(η^3-cyclooctenyl) (**11**) [ν(CO) = 2074 cm^{-1} assigned to the platinum carbonyl ligand]. On removal of CO (argon purge), **8a** is re-formed.

Preparation of (OC)$_4$Cr(μ-P^{n}Pr$_2$)(μ-H)Pt(CO)(PCy$_3$) (6d). Pt(C_2H_4)$_2$(PCy$_3$) (0.43 g, 0.807 mmol) was added to a dichloromethane (3 mL) solution of Cr(CO)$_5$(PPr$_2$H) (0.25 g, 0.807 mmol) at room temperature. After 1 h, the addition of pentanes (5–10 mL) affords yellow crystals. The mother liquor was decanted, and the crystals were washed with pentanes (3 × 5 mL) and dried in vacuo to give **6d** (0.50 g, 0.638 mmol, 79% yield). Complexes **6a–c, e,f** were similarly prepared in yields ranging from 60 to 80%.

Preparation of (OC)$_3$(PEt$_3$)Mo(μ-PPh$_2$)(μ-CO)PtH(PCy$_3$) (14a). Pt(C_2H_4)$_2$(PCy$_3$) (0.186 g, 0.35 mmol) was added to a stirred CH_2Cl_2 (5 mL) and pentane (10 mL) solution of Mo(CO)$_4$(PEt$_3$)(PPh$_2$H) (0.180 g, 0.35 mmol). Removal of solvent after the reaction is >90% complete (24 h, verified by IR) affords a red oil, which, upon rapid stirring in pentanes (15 mL; 25 min), gives **14a** as a bright yellow solid (0.276 g, 0.28 mmol, 80% yield). The tungsten analogue **14b** was prepared in a similar manner and yield.

Formation of 3f from the Reaction of W(CO)$_4$(PPh$_3$)(PPh$_2$Li) with PtHCl(PEt$_3$)$_2$. Methyllithium (1.9 M in Et$_2$O, 0.47 mmol) was added to a THF (10 mL) solution of W(CO)$_4$(PPh$_3$)(PPh$_2$H) (0.671 g, 0.90 mmol) at room temperature. After the mixture was stirred for ca. 5 min, *trans*-PtHCl(PEt$_3$)$_2$ (0.422 g, 0.90 mmol) was added. When the volume of the solution was reduced (under vacuum) to ca. 3 mL, yellow crystals of **3f** (0.50 g, 0.55 mmol) were obtained. Complexes **3e,h,i** were similarly prepared in ca. 60% yield.

X-ray Structure Determination of 3d and 8a. Crystals of **3d** (recrystallized from THF) were dark green rhombs; those of **8a** (recrystallized from CH_2Cl_2/hexane) were brown rhombs. Precession photographs were used to check crystal quality. Further work on an Enraf-Nonius CAD4 diffractometer using graphite-monochromatized Mo K$\bar{\alpha}$ radiation (λ = 0.71069 Å) gave the following summarized crystallographic data. Both structures were solved by the use of the Patterson function followed by standard least-squares and Fourier methods. Final atomic positional parameters for **3d** and **8a** are given in Table VI.

Summary of Crystallographic Data. 3d: $C_{28}H_{41}CrO_4P_3Pt$, monoclinic, space group *Cc*, a = 16.719 (9) Å, b = 11.468 (3) Å, c = 18.275 (6) Å, β = 113.68 (3)°, V = 3209 Å^3, D_x = 1.62 g cm^{-3} for Z = 4, T = 298 K, μ(Mo Kα) = 49.1 cm^{-1}. Intensity data collection (ω–2θ scans; octants $h,k,\pm l$ with $2\theta \leq 60°$; maximum scan time 85 s) gave 5759 data. *Lp* and absorption corrections (total 0.431 – 0.516) were made to all data. Full-matrix least-squares refinements ($\sum w\Delta F^2$ minimized) converged to R (R_w) = 0.0346 (0.0401) for 3801 reflections with $I \geq 3\sigma(I)$ (all non-H atoms anisotropic). Maximum $\Delta\rho$ = 1.37 e Å^{-3} near Pt. Least-squares refinement of the alternative "hand" gave R (R_w) = 0.0466 (0.0607). **8a**: $C_{25}H_{23}CrO_5PPt$, monoclinic, $P2_1/a$, a = 25.212 (3) Å, b = 10.172 (2) Å, c = 9.577 (2) Å, β = 90.53 (1)°, V = 2456 Å^3, D_x = 1.85 g cm^{-3} for Z = 4, μ(Mo Kα) = 62.9 cm^{-1}, T = 298 K. Intensity data collection (ω–2θ scans; octants h, k, $\pm l$ with $2\theta \leq 55°$; maximum scan time 90 s) gave 6436 data. *Lp* and absorption corrections (total 0.349–0.451) were made to all data. Full-matrix least-squares refinements converged to R (R_w) = 0.0329 (0.0382).

Acknowledgment. We are grateful to the Natural Sciences and Engineering Research Council of Canada for financial support of this work.

Registry No. 1a, 18399-60-5; **1b**, 18399-61-6; **1c**, 18399-62-7; **1d**, 123596-77-0; **1e**, 123596-78-1; **1f**, 123596-79-2; **2a**, 94283-18-8; **2b**, 94283-19-9; **2c**, 94283-17-7; **2j**, 94283-16-6; **2k**, 94283-15-5; **2l**, 94283-14-4; **2m**, 123596-86-1; **2n**, 123596-87-2; **2o**, 123596-88-3; **3a**, 94365-19-2; **3b**, 94365-20-5; **3c**, 94365-21-6; **3d**, 94365-15-8; **3e**, 94365-14-7; **3f**, 94365-13-6; **3g**, 123596-80-5; **3h**, 123621-22-7; **3l**, 123596-81-6; **3j**, 94365-16-9; **3k**, 94365-17-0; **3l**, 94365-18-1; **3m**, 123596-82-7; **3n**, 122412-46-8; **3o**, 122412-47-9; **4a**, 123596-83-8; **4b**, 123596-84-9; **4c**, 123596-85-0; **5**, 123596-89-4; **6a**, 122114-37-8; **6b**, 122093-91-8; **6c**, 122114-38-9; **6d**, 123273-06-3; **6e**, 123273-07-4; **6f**, 123273-08-5; **6g**, 123596-96-3; **6h**, 123597-01-3; **7a**, 123596-90-7; **7c**, 123596-91-8; **8a**, 123596-92-9; **8c**, 123596-93-0; **11a**, 123596-94-1; **11c**, 123596-95-2; **12**, 123596-97-4; **13a**, 123596-98-5; **13b**, 123672-46-8; **14a**, 123596-99-6; **14b**, 123597-00-2; **15a**, 123597-02-4; Pt(C_2H_4)(PPh$_3$)$_2$, 12120-15-9; Pt(C_2H_4)$_2$(PCy$_3$), 57158-83-5; Pt(COD)$_2$, 12130-66-4; *trans*-PtHCl(PEt$_3$)$_2$, 16842-17-4; *trans*-PtHCl(PMe$_2$Ph)$_2$, 12112-64-0.

Supplementary Material Available: Table S-I, containing crystal, intensity measurement, and structure refinement data, and Tables S-II and S-III, containing anisotropic thermal parameters and bond lengths and bond angles for **3d** and **8a** (10 pages); Table S-IV, containing final structure factor amplitudes for **3d** and **8a** (43 pages). Ordering information is given on any current masthead page.